FABRICATION OF SINGLE-WALLED CARBON NANOTUBE TRANSPARENT CONDUCTIVE THIN FILMS

M.Sc. THESIS

Fatma ÇOLAK

DECEMBER 2015

ISTANBUL TECHNICAL UNIVERSITY ★ ENERGY INSTITUTE

FABRICATION OF SINGLE-WALLED CARBON NANOTUBE TRANSPARENT CONDUCTIVE THIN FILMS

M.Sc. THESIS

Fatma ÇOLAK
(301121031)

Energy Science & Technology Division

Energy Science & Technology Programme

Thesis Advisor: Prof. Dr. Nilgün YAVUZ

DECEMBER 2015

İSTANBUL TEKNİK ÜNİVERSİTESİ ★ ENERJİ ENSTİTÜSÜ

GEÇİRGEN VE İLETKEN TEK DUVARLI KARBON NANOTÜP İNCE FİLMLERİN HAZIRLANMASI

YÜKSEK LİSANS TEZİ

Fatma ÇOLAK
(301121031)

Enerji Bilim ve Teknoloji Anabilim Dalı

Enerji Bilim ve Teknoloji Programı

Tez Danışmanı: Prof. Dr. Nilgün YAVUZ

ARALIK 2015

Fatma Çolak, a M.Sc. student of ITU Energy Institute student 301121031, successfully defended the thesis entitled "FABRICATION OF SINGLE-WALLED CARBON NANOTUBE TRANSPARENT CONDUCTIVE THIN FILMS", which she prepared after fulfilling the requirements specified in the associated legislations, before the jury whose signatures are below.

Thesis Advisor :　　**Prof. Dr. Nilgün YAVUZ**　　　.............................
　　　　　　　　　　　Istanbul Technical University

Jury Members :　　**Prof. Dr. Üner ÇOLAK**　　　.............................
　　　　　　　　　　Istanbul Technical University

　　　　　　　　　　Prof. Dr. Yeşim HEPUZER　　　.............................
　　　　　　　　　　Istanbul Technical University

Date of Submission : 3 November 2015
Date of Defense :　　18 December 2015

FOREWORD

I would like to express my sincere gratitude to my supervisor Prof. Dr. Nilgün YAVUZ for sparing so much of her time, advices and encouragements through the study. Without her guidance and support this work could not have been accomplished.
I would also like to thank Amin TABATABAEI and Ergin KÜKRER for their invaluable support.
Lastly and most importantly, I thank my family, for their love and never ending support of all my decisions.

November 2015
Fatma ÇOLAK
(Chemical Engineer)

TABLE OF CONTENTS

ABBREVIATIONS

CNT   **:** Carbon Nanotube
CVD   **:** Chemical Vapour Deposition
DI   **:** Deionized
DOS   **:** Density of States
FoM   **:** Figure of Merit
ITO   **:** Indium Tin Oxide
MCE   **:** Mixed Cellulose Ester
MWNT   **:** Multi-walled Carbon Nanotube
NMP   **:** N-Methyl-2-pyrrolidone
NW   **:** Nanowire
PEDOT: PSS : Poly(3,4-ethylenedioxythiophene) polystyrene sulfonate
SDS   **:** Sodium Dodecyl Sulfate
SEM   **:** Scanning Electron Microscopy
SWNT   **:** Single-walled Carbon Nanotube
TCF   **:** Transparent Conductive Film
TCO   **:** Transparent Conductive Oxide
TGA   **:** Thermogravimetric Analysis

LIST OF SYMBOLS

C_2H_2   **:** Acetylene
C_h   **:** Chiral vector
d   **:** Diameter
E_{gap}   **:** Energy gap
HNO_3   **:** Nitric acid
I   **:** Current
L   **:** Length
MgO   **:** Magnesium oxide
R   **:** Radius
R_s   **:** Sheet resistance
$SOCl_2$ **:** Thionyl chloride
T   **:** Primitive translation vector
V   **:** Voltage
W   **:** Width
θ   **:** Chiral angle

LIST OF TABLES

LIST OF FIGURES

FABRICATION OF SINGLE-WALLED CARBON NANOTUBE THIN FILMS

SUMMARY

The need for transparent conductive films is growing rapidly as electronic devices, such as touch screens, displays, solid state lighting, and photovoltaics become essential in our lives. Doped metal oxides, in particular industry standart indium tin oxide, are the most widely used materials for transparent conductors. However, these materials have several drawbacks, including a high refractive index and haze, spectrally nonuniform optical transmission, limited flexibility, and a depleted raw material supply and exploration of alternative materials has become inevitable.

Because of their high intrinsic carrier mobility, conductivity, and mechanical stability carbon nanotubes (CNTs) are promising materials for electronics, as transparent conductors. There are two commonly used methods for depositing SWNTs on substrates-transferring CVD-grown SWNTs or deposition of solution processed SWNTs. Since CVD grown SWNTs can be highly aligned, they often outperform solution-processed SWNT films that are typically in the form of randomly construcred networks. On the other hand, solution-based SWNTs can be printed at a large-scale and at low-cost, rendering them more appropriate for manufacturing.

In this thesis, transparent and conductive SWNT electrodes were fabricated on glass substrates. SWNTs were firstly synthesized by chemical vapor deposition of acetylene on Fe/MgO catalyst at 800°C and purified by 6M HNO_3 at 98.39 % purity level.

Spray coating method was utilized for the deposition of SWNTs. Effects of sonication time, density of SWNT films, dispersing media, CNT type and post-deposition acid treatments were investigated. Fabricated SWCNT thin films were characterized by scanning electron microscopy (SEM) and UV-vis spectrophotometer. Four point probe measurements were also performed for determination of the sheet resistance values of SWCNT thin films on glass substrates and the resultant properties were compared.

It has been found that, 195 Ω/sq sheet resistance can be achieved at an optical transmittance of 75 % for Tuball-SWNT thin films on glass substrates that were deposited via spray coating method. All of the fabricated films were found to be mechanically robust, with no tendency to delaminate from the underlying substrate.

GEÇİRGEN VE İLETKEN TEK DUVARLI KARBON NANOTÜP İNCE FİLMLERİN HAZIRLANMASI

ÖZET

Geçirgen ve iletken malzemelere olan rağbetin; dokunmatik ekran, katıhal aydınlatma ve fotovoltaik gibi elektronik uygulamaların hayatımızın vazgeçilmez bir parçası haline gelmesi ile hızlı bir şekilde artması beklenmektedir. Doplanmış metal oksitler, özellikle indium kalay oksit (ITO) en çok kullanılan geçirgen ve iletken malzemelerdir, fakat bu malzemelerin bazı dezavantajları, yeni ve alternatif malzemelerin geliştirilmesine yol açmıştır.

Endüstri standardı olan ITO kaplı camlar yalnızca pahalı değil, mekanik olarak da kırılgan yapıdadır. Aktif bir malzeme olan ITO, korozif malzemelerle reaksiyona girebilmektedir. En önemlisi de ITO'nun iletkenliğinin düşük olması güneş pili dolum faktörünü düşürmektedir.

Son yıllarda, ITO yerine kullanılabilecek elektrot malzemelerinin geliştirilmesi için yoğun çalışmalar yapılmaktadır. Gümüş nanoparçacıklar, nanoteller, grafen ve karbon nanotüpler bu malzemeler arasındadır. Karbon nanotüpler; üstün optik ve elektriksel özellikleri ile, ITO'nun yerine kullanılabilecek iyi bir alternatiftir.

Karbon nanotüpler, günümüzde nano teknolojinin vazgeçilmez unsurlarından olup yoğun olarak araştırılan malzemelerdir. Grafit plakasının kırvrılarak elde edilen silindir şeklindeki bu malzemelerin çapları birkaç nanometreyken uzunlukları milimetrelerle ifade edilebilir. Çaplarının milyonlarca katı uzunluklara ulaşabilen karbon nanotüpler, mekanik, kimyasal, ısıl ve elektriksel özelliklerinin çok iyi olmasıyla birlikte birçok farklı potansiyel uygulama için umut vaat eden eşsiz malzemelerdir.

Yüksek yük mobiliteleri, iletkenlikleri ve mekanik dayanımları gibi özellikler karbon nanotüplerin (KNT) elektronik uygulamalarda geçirgen elektrot olarak kullanımlarını gündeme getirmiştir. KNT'lerin istenilen yüzeye kaplanması için genellikle iki yöntem kullanılmaktadır. Bunlar, kimyasal buhar birikimi (KBB) yöntemi ile üretilen filmlerin doğrudan transferi ve çözelti bazlı yöntemlerdir. KBB yöntemi ile üretilen filmlerin hizalanabilmelerinden dolayı optoelektronik özellikleri çözelti bazlı kaplamalardan daha iyi sonuç vermektedir. Fakat çözelti bazlı yöntemlerin büyük ölçekli kaplamalara uygun ve maliyetlerinin düşük olması gibi avantajları bulunmaktadır. Ayrıca, karbon nanotüp ince filmlerin kaplama sürecinde vakum sistemine ihtiyaç yoktur ve çözelti bazlı kaplama yöntemleriyle düşük sıcaklıklarda çeşitli altlıklar üzerine geniş alanlara uygulanabilmektedir. Püskürtme ile kaplama tekniği, geniş alan uygulamalar için uygun kaplama yöntemidir. Geçirgen elektrot uygulamalarında da tek duvarlı karbon nanotüp ince filmler, pratik püskürtme ile kaplama yöntemiyle kolaylıkla oluşturulabilir.

Çözelti bazlı yöntemlerde homojen KNT çözeltisinin elde edilmesi en önemli adımdır. Çözücünün seçimi ve KNT konsantrasyonu dışında, karıştırma tekniği, hızı ve süresi gibi etmenlerin optimizasyonu çok önemlidir. KNT yoğunluğunun bir başka deyişle KNT miktarının yüksek olması geçirgenliğin azalmasına ve yüzey direncinin artmasına; düşük olması ise iletkenliğin azalmasına sebep olmaktadır. Bu

nedenle, en uygun KNT yoğunluğu belirlenmelidir. Ayrıca, karıştırma tekniğine göre uygun güç ve sürede karıştırma işlemi yapılmalıdır. Karıştırıcının düşük güçte olması ya da yeterli süre uygulanmaması karbon nanotüplerin karışmamasına, yüksek güçte uzun süre karıştırılmaları ise karbon nanotüplerin zarar görmelerine sebep olmaktadır. Her iki durumda da yüzey dirençleri artmaktadır.

Geçirgen ince film yüzeyinde, karbon nanotüpler rastgele dağılmış ağ şeklinde bir yapı oluşturmaktadır. Bu yapının iki önemli özelliği, yüzey direnci ve optik geçirgenliktir. Her iki özellik de film kalınlığına bağlı olarak değişebilir. Çoğu uygulamalarda yüksek geçirgenlik ile düşük yüzey direnci gereklidir. Ancak bazı özel uygulamalarda bu gereksinimden uzaklaşılabilmektedir. Genel olarak istenen geçirgenlik elde edildikten sonra yüzey direncinin düşürülebilmesi için asit ile muamele, ısıl işlem gibi çeşitli yöntemler uygulanmaktadır. Asit ile muamele, kaplama yüzeyinden istenmeyen maddeleri uzaklaştırmakla birlikte, KNT'leri p-tipi doplayarak filmlerin yüzey direncini düşürülmektedir.

Tez çalışması kapsamında, tek duvarlı karbon nanotüpler (TDNT) kullanılarak geçirgen elektrotlar üretilmiştir. İlk olarak, tek duvarlı karbon nanotüpler, kimyasal buhar birikimi yöntemine göre demir katalizörü ve asetilen gazı kullanılarak 800 °C'de sentezlenmisler ve 6M HNO_3 ile saflaştırılmışlardır (% 98.39). Tek duvarlı karbon nanotüplerin cam yüzey üzerine kaplanmasında, sprey kaplama yöntemi kullanılmıştır. Sonikasyon süresi, çözücü ortam, KNT türü ve kaplama sonrası asit işlemin etkileri incelenmiştir. Üretilen TDNT ince filmler, taramalı elektron mikroskobu (SEM) ve UV-vis spektrofotometre ile karakterize edilmiştir. Dört nokta direnç ölçüm cihazı ile farklı parametrelerle üretilen ince filmlerin yüzey dirençleri tespit edilmiş ve karşılaştırılmıştır.

Tez çalışmasında, püskürtmeli kaplama yöntemi ile geliştirilen KNT filmlerin homojen bir şekilde cam yüzeylere kaplandığı ve mekanik özelliklerinin de iyi olduğu görülmüştür.

Homojen KNT çözeltisinin hazırlanması için sonikasyon süresi optimize edilmesi gereken en önemli parametrelerden bir tanesidir. 60 ve 120 dakika olmak üzere iki farklı sonikasyon süresinin ince filmlerin optoelektronik özelliklerine etkisi incelenmiş ve 60 dakikalık sonikasyon süresinin yeterli olduğu tespit edilmiştir. Sürenin artması ile KNT'lerin yüzeylerindeki kusurlar artmakta ve dolayısıyla elektronik özellikleri kötüleşmektedir.

Kaplanan KNT'lerin yoğunluğu bir diğer önemli etkendir. Film yoğunluğu arttıkça, yüzey direnci iletim yollarındaki artış sebebiyle düşmekte, fakat geçirgenlik azalmaktadır.

Dispersiyon ortamının etkisinin araştırılması için organik çözücü ve yüzey aktif maddenin sulu çözeltisi olmak üzere iki farklı çözelti hazırlanmış ve cam yüzeylere kaplanmıştır. Geçirgen ve iletken filmlerin optoelektronik özelliklerine bakıldığında yüzey aktif maddenin kullanılması ile hazırlanan filmlerin daha iyi performans sergilediği ve mekanik dayanımlarının daha yüksek olduğu tespit edilmiştir.

KNT türünün etkisinin incelenmesi için KBB yöntemiyle laboratuvarımızda ürettiğimiz TDNT'ler ile OCSiAl şirketinden temin edilen Tuball TDNT'ler aynı koşullarda dispers edilmiş ve cam yüzeylere kaplanmıştır. Tuball-TDNT'ler kullanılarak hazırlanan filmlerin, %75 geçirgenlikte yüzey dirençlerinin 195 Ω/kare'ye kadar düşürülebildiği görülmüştür. KBB yöntemi ile üretilen TDNT'lerin ise yüzey dirençleri, benzer geçirgenlikler için, yaklaşık olarak 1000 kat daha yüksek bulunmuştur. KNT'lerin kristal yapılarının kalitesi arasındaki fark bu durumun başlıca sebebi olarak görülebilir.

Üretilen KNT ince filmlerinin elektronik özelliklerinin iyileştirilmesi için filmler, kaplama sonrasında asite daldırılmış ve 30 dakika boyunca bekletilmiştir. Yapılan ölçümler, filmlerin yüzey dirençlerinin önemli ölçüde düştüğünü ortaya çıkarmıştır. Bunun sebebi asitle muamele sonucunda yarı-iletken KNT'lerin p-tipi doplanması ve serbest yük taşıyıcı konsantrasyonunun artması olarak gösterilebilir.

1. INTRODUCTION

Nanomaterials, defined as having at least one dimension less than 100 nm, have been receiving growing interest due to their unique properties, mostly superior to their bulk counterparts. Zero-dimensional nanoparticles, one-dimensional nanowires, and two-dimensional (2D) graphenes can be included as typical examples. Novel electrical, optical, and magnetic properties can be achieved in nanostructures because of the quantum confinement of electrons in one or more dimensions [1].

Carbon nanotubes (CNTs) are one of the most promising materials among nanoscale materials. Nanotubes can be thought of as rolled graphene sheets and exist both as single-walled nanotubes (SWCNTs) and as multi-walled nanotubes (MWCNTs). Depending on the chirality along the graphene sheet, SWNTs exhibit either semiconducting or metallic behaviour. Both experiments and theory have shown that SWCNTs possess high mobility (on the order of 100,000 $cm^2V^{-1}s^{-1}$), high conductivity (up to 400,000 Scm^{-1}), and, for semiconducting nanotubes, tube diameter-dependent band gap ($E_{gap} \approx 1/R_{tube}$) [1].

Transparent conductive films (TCFs) are widely used in industry, especially in optoelectronic aplications because they are electrically conductive and optically transparent into visible light range. TCFs are essential components for liquid crystal displays (LCDs), organic light emitting diodes (OLEDs), organic photovoltaic (OPV) cells and touch panels, etc. A market research report at ReportsnReports.com shows that the touch panel TCF market is $956 million in 2012 and is anticipated to reach $4.8 billion by 2019, indicating that TCFs have a tremendous marketplace. With the rapid development and upgrading of consumer electronics such as e-readers and smart phones, not only the demand for TCFs is growing fast, but also their properties need to be significantly improved [2].

Currently, indium tin oxide (In_2O_3:Sn, ITO) is the industry standart TCF material due to its excellent opto-electrical properties with low sheet resistance, R_s, of 10–25 Ω/sq at about 90% transparency.

Although current optoelectronic devices are commonly assembled on glass substrates, flexible versions are becoming a developing trend, especially in academic researches, and will open new applications and markets. In addition to being conductive and transparent, flexible optoelectronic applications require cost effective and large scale competible manufacturing methods [3]. Considering the advancement of optoelectronic devices, ITO has several drawbacks: (i) it is becoming increasingly expensive due to the predicted shortage of indium resources and its ever-rising consumption; (ii) the deposition of ITO requires vacuum procedures and often elevated temperatures; (iii) it lacks flexibility and cracks easily, which limits its use for flexible electronics; (iv) indium is known to diffuse into the active layers of OLEDs or OPV cells, which leads to a degradation of device performance [4]. Therefore, in order to keep the pace of device development, new alternative materials are urgently needed to replace ITO-TCFs.

In recent years, many efforts have been made to develop ITO alternatives. TCFs have been fabricated by using CNTs and graphene, conducting polymers, the most promising being poly(3,4-ethylenedioxythiophene) poly(styrenesulfonate) (PEDOT:PSS), metal grids and random networks of metallic nanowires (NWs). Some hybrid TCFs based on CNT/PEDOT:PSS, graphene/PEDOT:PSS and CNT/graphene, etc., are also being developed. Although conducting polymers are extremely flexible, they have the disadvantages of poor stability and a noticeable blue color [5]. The electrical properties and transparency of metallic NWs or grids can out-perform ITO electrodes on plastic substrates, [6] but their haze makes them incompatible with many display applications [5]. Also environmental stability and scalable fabrication are some of their main problems. Among these alternative materials, CNT-TCFs have been extensively investigated due to their unique optoelectronic and mechanical properties. Using CNTs as TCFs brings multiple advantages: (i) carbon is a cheap, abundant material and can meet the increasing demand of devices for transparent electrodes. (ii) CNTs are much stronger and more flexible than ITO. (iii) CNTs have shown solution processability and have potential for low cost production. (iv) CNTs are chemically stable, which is beneficial for a longer device life. (v) CNT-TCFs have a neutral color and wide transmittance spectrum range, which is significant for most applications including OPV cells, OLEDs and displays. As a result, CNTs have been considered as ideal transparent

electrodes for optoelectronic devices. Therefore, TCFs have been identified to be one of the most promising field for the industrial applications of CNTs [2].

Fabrication of SWNT thin films can be achieved by direct growth or solution based deposition techniques such as vacuum filtration, spin coating, dip coating or spray coating. Solution based deposition techniques are cost effective and applicable over large areas and various substrates, but they require homogeneous SWNT dispersions. SWNTs have large aspect ratio; thus, they easily agglomerate in the form of bundles due to van der Waals interactions. Dispersion process includes sonication steps for neat solvent or surfactant aided SWNT solutions. Sonication activates the unzipping behavior of the SWNT bundles. However, sonication type, time, and power can damage and shorten SWNTs due to heat generation during the process. Optimization of sonication and dispersion parameters directly affect the stability of the dispersion and the SWNT thin film quality.

Doping of CNT thin films is essential step for further performance improvement and modifications. This process increases the delocalized carrier density, while lowering the intertube conduction barrier resulting in conductivity improvement for TCFs.

Chapter 2 presents the properties of CNTs from different aspects in detail. Crystal structure, electronic and optical properties of CNTs were given to understand the extraordinary properties of this 1D material.

Chapter 3 investigates SWCNT thin film fabrication processes from many viewpoints including dispersion, deposition and post-deposition treatments in detail. Furthermore evaluation of thin film properties was also examined in detail.

Chapter 4 presents the experimental studies performed at this work. It includes CNT synthesis, thin film fabrication and characterization.

Chapter 5 offers the results of CNT synthesis, thin film preparation and characterization. It includes evaluation of thin films fabricated via spray coating method at different conditions.

The overall results and recommendations for this study are given in Chapter 6.

2. CARBON NANOTUBES

2.1 Carbon Allotropes

The element carbon is the fourth most abundant element in the solar system, after hydrogen, helium, and oxygen, and is found mostly in the form of hydrocarbons and other compounds.

Carbon is the basic constituent of all organic matter and the key element of the compounds that form the huge and very complex discipline of organic chemistry. Carbon is different from other elements in one important respect, that is its diversity which can be attributed to the ability to form different bonds [7].

Carbon can have different and important properties depending on its bonding structure and possible atomic configuration. Each carbon atom has six electrons, occupying $1s^2$, $2s^2$, $2p^2$ orbitals. Electrons occupying $2s^2$ and $2p^2$ orbitals are valence electrons which can form different covalent bonds depending on the hybridization type. Common carbon allotropes such as diamond, graphite, nanotubes of fullerenes have different bonding structure due to different hybrid orbitals as shown in Figure 2.1.

sp^3 hybrid structure, demonstrated in Figure 2.1 (a), has a tetrahedral geometry and composed of three p orbitals and one s orbital, forming strong covalent sigma (σ) bonds. sp^2 hybridized atoms shown in Figure 2.1 (b) have trigonal geometries combining the s orbital with two p orbitals and forming σ bonds, while other two p orbitals are forming pi (π) bonds. sp hybrid structure is a combination of one s and one p orbital which has a linear geometry as shown in Figure 2.1 (c).
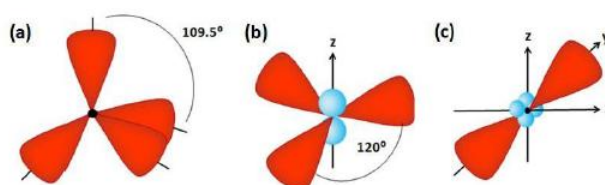
Figure 2.1 : (a) sp^3, (b) sp^2, (c) sp hybridized carbon atoms.

Diamond has a tetrahedral crystal structure and each sp^3 hybridized carbon atom is bonded to four other atoms with σ bonds, as shown in Figure 2.2 (a). Diamond is the hardest (Mohs hardness 10), naturally occurred material because of this firmly constructed arrangement. Diamond is a wide gap semiconductor (5.47 eV) and has the highest thermal conductivity ($\sim$25 Wcm^{-1}K^{-1}) and the highest melting point (4500 K).

Graphite is another carbon allotrope, which consists of the sp^2 hybridized atoms. In each carbon atom, three of the four outer shell electrons are hybridized to sp^2 orbitals and form strong covalent σ bonds with the three neighbouring carbon atoms [8]. The remaining valence electron in the π orbital provides the electron band network that is largely responsible for the charge transport in graphene [9]. This bonding structure forms a planar hexagonal network like a honeycomb as shown in Figure 2.2 (b). Monolayer is called a graphene sheet and layers are held together by van der Waals forces. The spacing between two graphene layers is 0.34 nm. Graphite conducts both electricity and heat due to its π bond electrons, which are free to move. Owing to its weak π bonds and the van der Waals interaction between the layers, graphite is a perfect lubricant hence the graphene sheets are able to glide away [10].

A spherical fullerene molecule, C60, is demonstrated in Figure 2.2 (c). C60 molecules are icosahedrals, composed of 20 hexagons and 12 pentagons forming a stable football like structure. Fullerenes are not planar, they have curvatures with some sp^3 character present in the essentially sp^2 hybridized carbons [11]. They have novel properties and so far utilized in electronic, magnetic, optical, chemical, biological and medical applications.
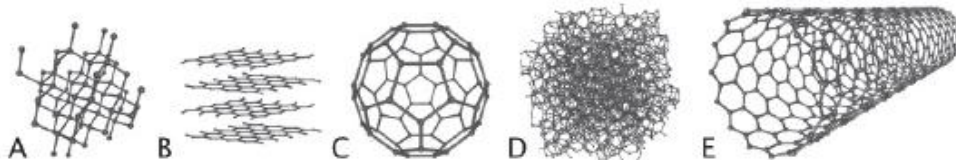
Figure 2.2 : Different allotropes of carbon (a) diamond (b) graphite (c) C60 fullerene (d) amorphous carbon (e) single-walled carbon nanotube.

CNTs are cylindrical nanostructures and formed by rolling of the graphene sheets. They can be open ended or their ends may be capped with bisected of fullerene as shown in Figure 2.2 (d). The sp^2 hybridization, which is the characteristic bonding of

graphite, has a significant effect on the formation of the CNTs. Bonding in CNTs fundamentally depends on the sp^2 hybridization, which makes them stable; whereas, the hallow cylindrical part is more strong than the ends of the CNTs due to the presence of sp^3 bonding in the end caps [12].

2.2 Carbon Nanotubes

CNTs were firstly described as "helical microtubules of graphitic carbon" by S. Iijima in 1991 [13], and then they became one the most important materials in nanotechnology. Their unique properties have attracted a lot of interest from researchers over interdisciplinary fields. Two years after the discovery of multi walled carbon nanotubes (MWNTs), single walled carbon nanotubes (SWNTs) were also observed in 1993 [14].

The bonding structure of CNTs, as mentioned in 2.1, is mostly composed of sp^2 bonds and they are found to have many extraordinary properties. CNTs have diameters within the nanometers range; but, they can be up to hundreds of micrometers long [12]. The difference gives them high aspect ratios, which could be as much as 1000:1.

Although CNTs are closely related to a two dimensional (2D) graphene sheet, their cylindrical symmetry and the quantum confinement in the peripheral direction makes them different from the graphene sheets. Electrons propagate only along the tube axis and electron transport takes place on this axis because of the quantum confinement. Thus, the electronic properties of the CNTs are originated from their 1D nature [15].

2.2.1 Structure and chirality of SWNTs

Single wall carbon nanotubes (SWCNT) can be described as the fundamental structural unit of nanotube with one atom thick wall. As shown in Figure 2.3, the structure of a SWCNT is explained in one dimensional unit cell formed by rolling an infinite sheet of graphene having a diameter size distribution of 1-2 nm [12]. SWCNTs are generally found in hexagonal crystal structure bundles which are attracted to each other by Van der Waals bonds and can have 100-500 SWCNTs [16]. A SWNT can be formed along different rolling directions. These different rolling directions, named chirality, impact their electronic properties and make SWNTs interesting electrical materials.
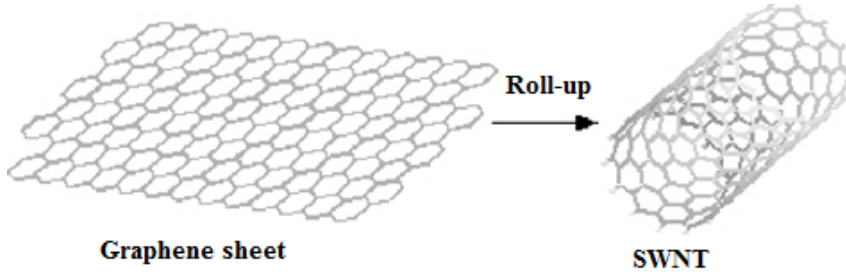
Figure 2.3 : Illustration of SWCNT.

SWNTs can be either semiconducting or metallic due to their chirality. A chiral vector along the circumference, $\vec{C}_h$, can be used to determine the possible wrapping angles. There are two integers, *n* and *m*, which are used as indices to describe chiral vector as,

$$\vec{C}_h = n\vec{a}_1 + m\vec{a}_2 \qquad (2.1)$$

where $\vec{a}_1$ and $\vec{a}_2$ are the graphene lattice vectors and $\vec{C}_h$ is a linear combination of these unit vectors as demonstrated in Figure 2.4. *n* and *m* are making a positive set of integers, which satisfies that $n > m$. Basically, $\vec{C}_h$ makes a connection between two sites of the graphene sheet. Chiral angle, θ, is the angle between $\vec{a}_1$ and $\vec{C}_h$. $\vec{T}$ is the translational vector along the tube axis. Chiral vectors of SWNT models are shown with the dark lines in Figure 2.4.
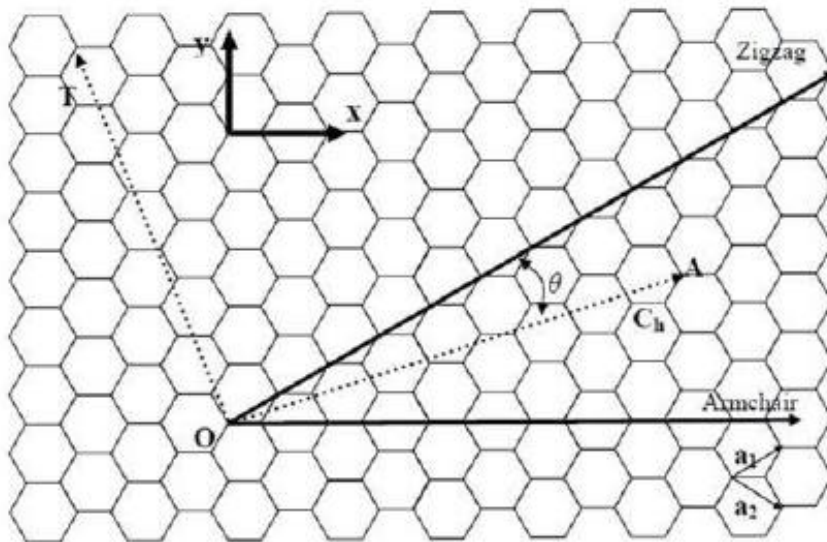
Figure 2.4 : Unit cell of a CNT.
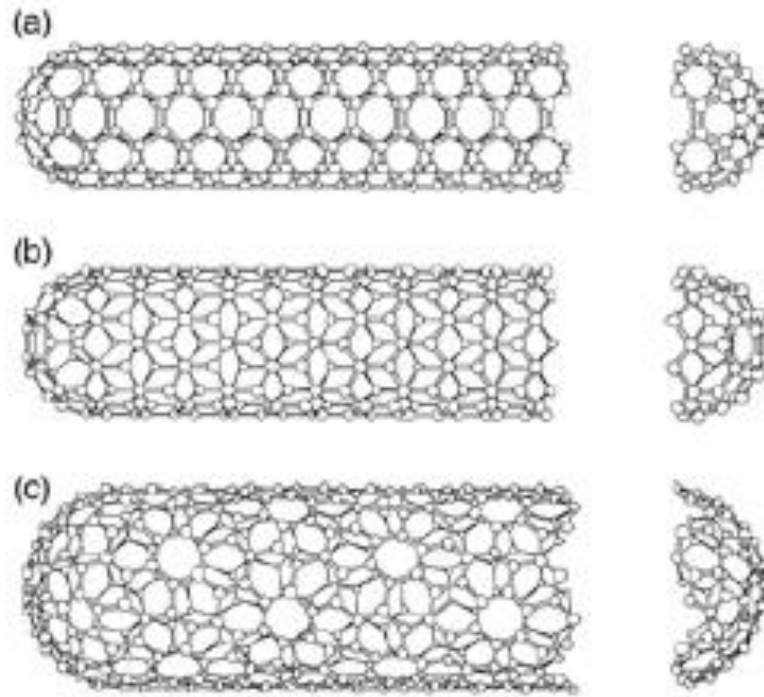
Figure 2.5 : a) armchair (*n,n*) b) zizag (*n,0*) c) chiral (*n,m*) nanotubes.

When a graphene sheet rolled with a chiral angle of θ, a (*n,m*) carbon nanotube is formed. There are different types of carbon nanotubes depending on (*n,m*) values as shown in Figure 2.5 [17]. (*n,0*) nanotube with a chiral angle of 0° is called zigzag nanotube, (*n,n*) with a chiral angle of 30° is called armchair nanotube and if *n* is different from *m* and chiral angle is between 0° and 30° then it is called chiral nanotube.

In a zigzag SWNT, *m* is zero because the chiral vector is parallel to $\vec{a}_1$ so the integer set will be always (*n*, 0). On the other hand, the chiral vector of an armchair model is the sum of $\vec{a}_1$ and $\vec{a}_2$ that makes the integers equal (*n=m*) and the set will be like (*n*, *n*).

Possible chiral vectors are given with their integer couples (*n,m*) and shown on a honeycomb graphene lattice in Figure 2.6, which confirm the zigzag structure has the integer pairs as (*n,0*) and the armchair structure is formed by the specified (*n,n*) pairs. All other tubes (*n,m*) are classified as chiral. (*n,m*) indices determine whether SWNTs are metallic or semiconducting, as well as their energy band gaps. If the difference between *m* and *n* is equal to the multiples of three, the nanotube is metallic

[18]; otherwise the tube is semiconducting and has a band gap value of 0.4 - 0.7 eV [19].

Figure 2.6 : Graphene network showing all the possible indices.

Diameter of the carbon nanotube, d_t and the chiral angle, θ depending on (n,m) values are given as,

$$d_t = \frac{1}{\pi} a \sqrt{n^2 + m^2 + mn} \qquad (2.2)$$

$$\sin \theta = \frac{\sqrt{3}}{2} \frac{m}{\sqrt{n^2 + m^2 + mn}} \qquad (2.3)$$

2.2.2 Electronic properties of SWNTs

Electronic properties of SWCNTs are dependent on their structure and can be metallic, semimetallic or semi-conductive with a band-gap of approximately 0.7 eV / d (nm) [12]. When a graphite sheet is rolled to form CNT not only the carbon atoms are ordered around the circular structure but also quantum mechanical wave functions of the electrons are ordered accordingly. The electrons are bounded in radial directions by the single layered graphite sheet. There exist periodical boundary conditions around the circle of the nanotube. If there are ten hexagons around

nanotube then the eleventh hexagon fits to first hexagon. As a result of the quantum boundaries the electrons are effective only along the nanotube axis enabling the determination of the wave vectors. Thus small diameter nanotubes are either metallic or semiconductors.

According to their electrical properties nanotubes can be classified as large gap, tiny gap and zero gap nanotubes. Theoretical calculations show that electrical properties of nanotubes depend on geometric structure. Graphene is a zero gap semiconductor, according to the theory carbon nanotubes can be metals or semiconductors having different energy gaps depending on diameter and helicity of nanotubes. As the nanotube radius R increases the band gap of large gap and tiny gap nanotubes decrease with $1/R$ and $1/R^2$ dependence, respectively [20-21]. The electrical properties of SWCNTs depend on n and m values: If $n = m$; formed armchair nanotube is metallic, If $n - m = 3k$, $k \in Z - \{0\}$ there are states at the corners of the first Brillouin zone and the tubes are semimetallic with a small, curvature induced band-gap of order of 100 meV. If $n - m = 3k \pm 1$, $k \in Z - \{0\}$ the nanotube is semi-conductive and exhibit diameter dependent band-gap.

2.2.3 Optical properties of SWNTs

Optical properties of carbon nanotubes derive from electronic transitions within one-dimensional density of states (DOS). A typical feature of one-dimensional crystals is that their DOS is not a continuous function of energy, but it descends gradually and then increases in a discontinuous spike (Figure 2.7).
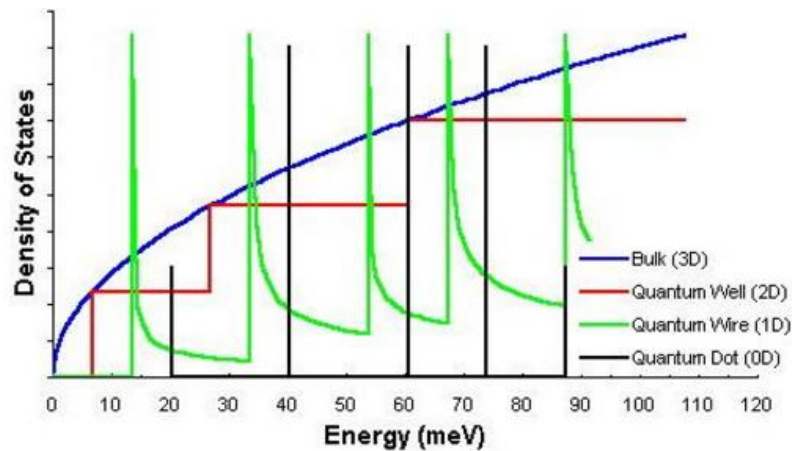
Figure 2.7 : Density of States of 1,2 and 3D materials.

11

The sharp peaks found in one-dimensional materials are called Van Hove singularities (Figure 2.8) and result in the remarkable optical properties of carbon nanotubes. The energies between the Van Hove singularities depend on the nanotube structure. Thus by varying this structure, optoelectronic properties of carbon nanotube can be tuned [22].
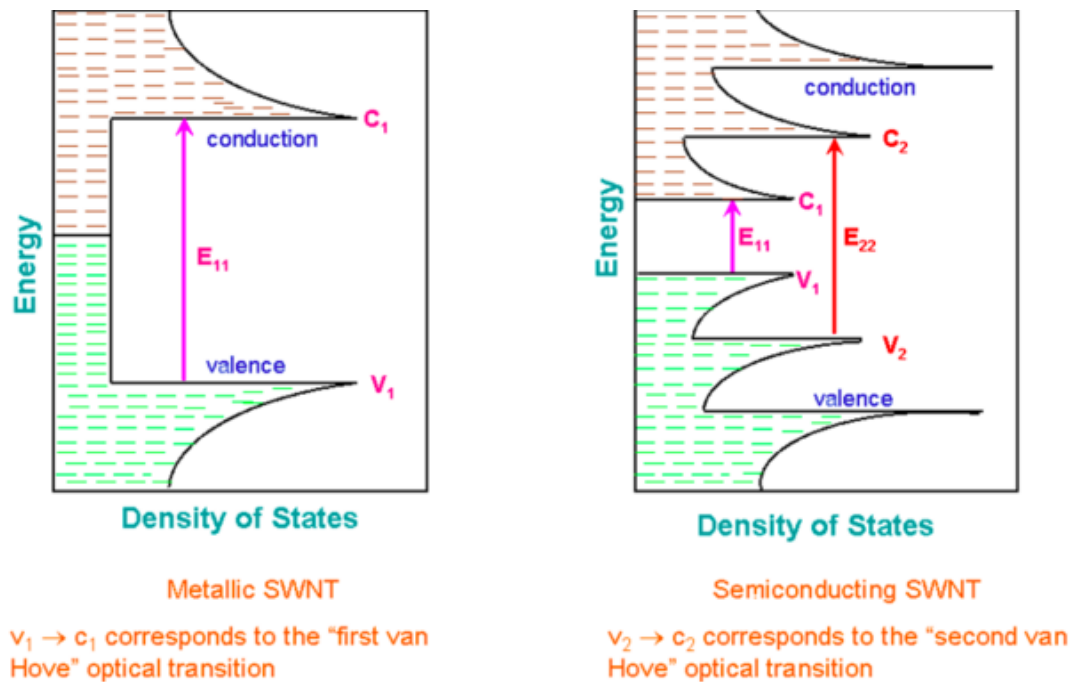
Figure 2.8 : Optical transitions of metallic and semiconducting SWNTs.

Optical properties of carbon nanotubes refer specifically to the absorption, photoluminescence (fluorescence), and Raman spectroscopy of carbon nanotubes.

The typical SWCNT absorption spectrum contains multiple characteristic peaks in range between 200-2600 nm. First, the metallic tubes contribute to M_{11} transition, which originates from transitions between the edges of the joint density of states of the metallic SWCNT. The semi-conducting tubes generate two distinct peaks, namely E_{11} and E_{22}, which correspond to the two lowest transitions between the van Hove singularities [23].

The optical absorption spectra can be used for SWCNT diameter distribution estimation. In typical samples which contain a mixture of SWCNTs, all the transitions are visible and the peaks are significantly broadened. For the characterization of the optoelectrical performance of SWCNT TCFs, transmittance at 550 nm wavelength is typically used [1].
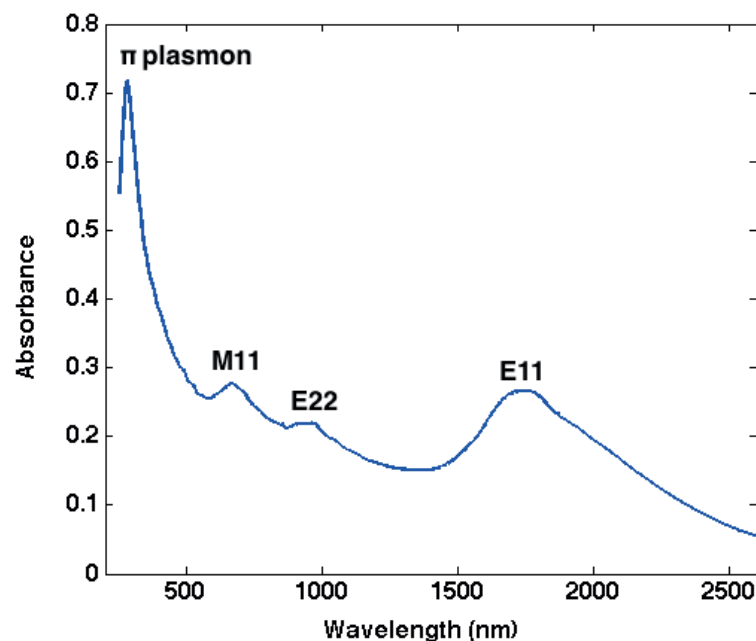
Figure 2.9 : The typical absorption spectrum of a SWCNT sample.

Raman-spectroscopy is another widely used technique for the characterization of SWCNTs. It is based on the inelastic scattering of photons due to the interaction between the optical field and the optical phonons [24]. It can be used for estimation of SWCNT diameter, band-structure and the number of defects. Due to the resonant nature of this technique, only the tubes whose band-gap is in resonance with the excitation laser wavelength are active, thus meaning that the complete Raman-characterization of a SWCNT sample requires a multi-source or a tunable laser system [25].

2.3 Synthesis of Carbon Nanotubes

As CNTs have wide range of applications, the growth techniques which can sustain high purity, and more amount of CNT becomes crucial. CNT synthesis can be achieved by different methods such as Arc discharge, laser ablation and Chemical vapour deposition (CVD).

2.3.1 Arc discharge

In 1991 Iijima reported formation of carbon nanotubes with arc discharge method which was previously used for production of fullerenes [13]. The tubes were produced having diameters ranging from 4 to 30 nm and having lengths up to 1µm.

13

In arc discharge method as shown in Figure 2.10 a direct current electric arc-discharge is produced in inert gas atmosphere by using two graphite electrodes [8, 14]. The CNTs grow on the negative end of the carbon electrode which produces the direct current while Argon as inert gas passes through the system. In arc discharge method a power supply of low voltage (12 to 25 V) and high current (50 to 120 A) is used. Catalyst, Ar:He gas ratio, the distance between the anode and the cathode, the overall gas pressure are the other parameters affecting the quality and the properties (i.e. diameter, yield percent) of CNT synthesised by arc discharge method [26-27].
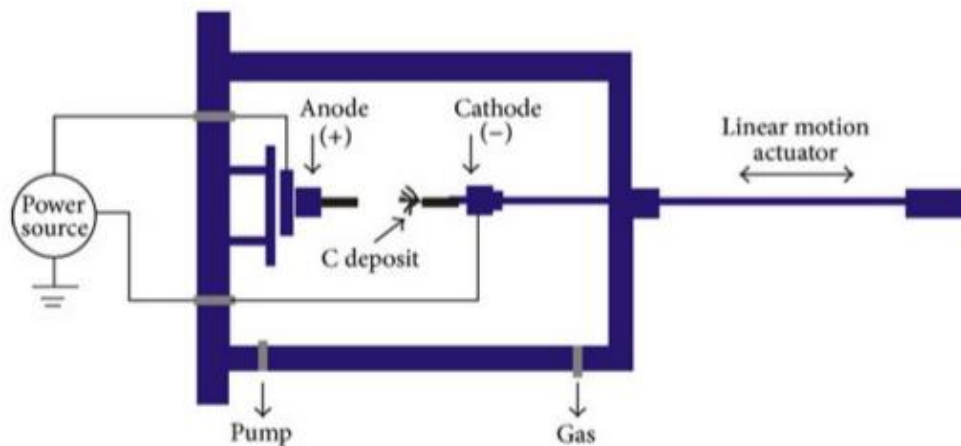
Figure 2.10 : Diagram of arc discharge method.

The positive electrode is consumed in the arc discharge gas atmosphere (i.e. Ar, He) CNT bundles are formed on the negative electrode. Length of MWCNTs produced by this method are generally around 1μm having a length to diameter ratio (aspect ratio) of 100 to 1000. As a result of high aspect ratio and small diameter of the produced MWCNTs they are classified as 1D carbon systems.

It has been reported that existence of catalyst (i.e. Fe, Co etc.) is required in the production of SWCNTs by arc discharge method [14,28]. Many catalyst composition can produce MWCNTs but it is observed that Y and Ni mixture yield up to 90% with an average diameter of 1.2 to 1.4 nm [29].

2.3.2 Laser ablation

Laser ablation method is very similar to arc discharge method as it also uses a metal impregnated carbon source to produce SMNT and MWNT [30]. In this method Co to Ni atomic percent of 1.2% and 98.8% of graphite composite in an inert atmosphere around 500 Torr of He or Ar in a quartz tube furnace of 1200ºC [31]. With the

treatment of pulsed or continuous laser light, the nano sized metal particles are formed in the vaporized graphite and these particles catalyse the growth of SWNT and by products. These products are condensed on the cold finger downstream of the source as shown in Figure 2.11. Smiley group in Rice University achieved the first large scale production of SWNTs by laser ablation method in 1996. The production yield of weight was varying between 20 to 80% SWCNTs. The diameters of produced SWCNTs were between 1.0 to 1.6 nm.
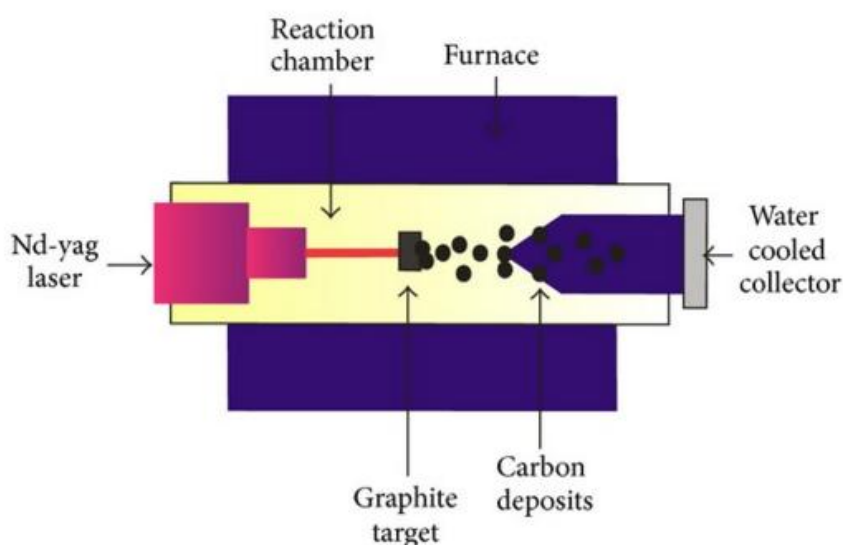
Figure 2.11 : Schematic view of laser ablation furnace.

2.3.3 Chemical vapour deposition

Different from laser ablation and arc discharge methods, chemical vapour deposition (CVD) which is a thermal synthesis method depends on a thermal source to produce CNTs by breaking down the carbon source generally with existence of catalysis [31]. High pressure CO synthesis, flame synthesis, CVD and plasma enhanced chemical vapour deposition (PECVD) synthesis are methods using thermal source to produce CNTs.

CVD method is deposition of a hydrocarbon gas as carbon source (i.e. acetylene, methane etc.) on a metal catalyst (i.e. Fe, Co, Ni, Pd etc) at temperatures between 500 and 1200 ºC. CVD has been used for production of nanofibers for long time [32]. This method is preferred for CNT syntheses because of high purity and large scale production [31, 33, 34]. CVD which was first reported to produce MWNTs by

Endo et al., can synthesise both SWNTs and MWNTs [35]. The main challenges in CNT production is to maintain mass production and low cost. In this respect, the catalytic method is claimed to be the best because of lower reaction temperatures and cost [36]. The amorphous carbon fomed as by product during the thermal decomposition of hydrocarbons can be eliminated by purification.

CNT production by CVD can either be on a fixed or fluidized bed reactor. In fixed bed CVD method as shown in Figure 2.12, the furnace placed horizontal to the ground and the quartz tube is placed in it [37]. The substrate material (MgO, alumina, zeolite etc.) coated with a catalyst (Fe, Co, Ni, Ag, Ti, etc.) is placed in the quartz tube and fed by a carbon source (i.e. hydrocarbons). Generally, an inert gas is used to maintain continuous gas flow. There are a number of parameters affecting the quality and amount of CNTs synthesised by CVD method:

- Temperature

- Type and amount of the catalyst material

- Type and amount of the substrate material

- Gas flow rate

- Duration of the synthesis

- Diameter of the reactor
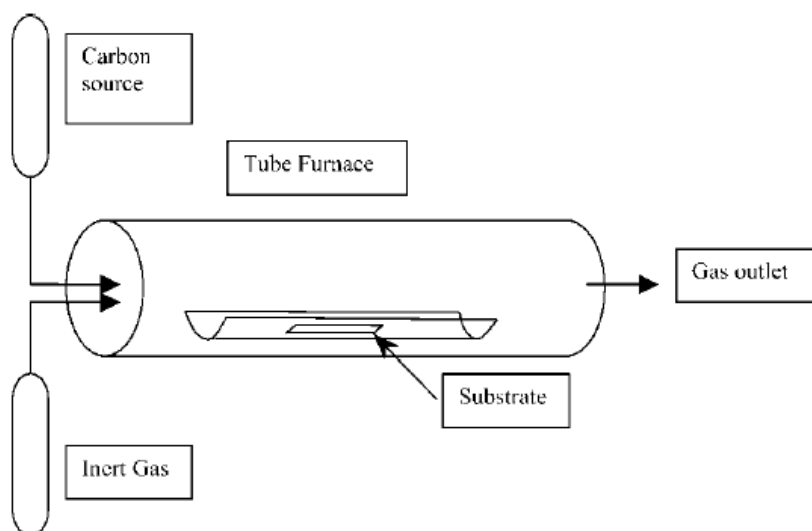
Figure 2.12 : Schematic view of fixed bed CVD reactor.

In fluidised bed CVD method as the interaction area of the carbon source gases and the catalyst increases with fluidisation, large scale production becomes possible. As shown in Figure 2.13 in this method the furnace is placed vertical to the ground and the quartz reactor is located in it. The substrate and catalyst couple is placed in the middle of the reactor in the hot zone of the furnace is placed in the hot zone of the furnace, and the gas flow through the reactor is maintained. As the carbon source gas flows through the reactor, it interacts with the catalyst and substrate and decomposes it for CNT synthesis.
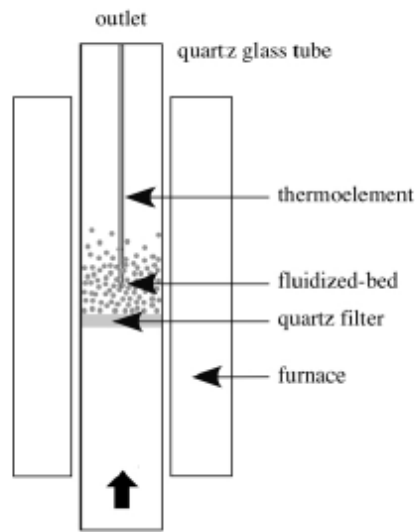
Figure 2.13 : Schematic view of fluidised bed CVD reactor.

3. CARBON NANOTUBE THIN FILMS

3.1 Fabrication of Carbon Nanotube Thin Films

There are two basic approaches for fabrication of CNT-TCFs, which are dry processes and wet (solution-based) processes. The difference between these two routes is whether CNTs need to be dispersed in solvents before their deposition on substrates.

Dry processes are based on direct growth of CNTs on substrate or membrane by CVD and it can be achieved by two different routes: (i) floating catalyst chemical vapor deposition (FCCVD) to produce a CNT aerosol and (ii) fixed catalyst chemical vapor deposition to produce a superaligned CNT (SACNT) array. Films produced by direct growth method are highly conductive due to better CNT-CNT contacts and also networks of individually separated tubes with fewer defects are formed during the growth [2].

Recently, solution-based film coatings have found widespread interest in both industry and academia, because they have several advantages over direct growth methods. Wet processes do not require high temperature or vacuum system, and they are also compatible with plastic substrates, which reduces cost significantly; and the deposition occurs at high speeds. Significant work has been published for CNT thin film applications. CNT material quality, CNT ink stability and degree of CNT dispersion are the crucial factors to achieve highly conductive CNT films [1].

There are several deposition routes and each of them has their own advantages and disadvantages. The most widely used solution based methods can be listed as, vacuum filtration, spray coating, spin coating and dip coating.

3.1.1 Dispersion

CNT ropes are bundles of individual CNTs aggregated together due to the high aspect ratio, large specific surface area, and strong van der Waals attraction between tubes. Furthermore, CNTs have inert surface to most common solvents, so the

attraction between CNTs is hard to overcome, which results in poor dispersion or even re-aggregation.

Carbon nanotubes (CNTs) can be dispersed in solution via three main ways: dispersion in organic solvents [38], dispersion in aqueous media via dispersing agents like surfactants [39–42] and dispersion in solution by functionalizing the CNTs [43-44].

Direct dispersion of CNTs in organic solvent is a simple and straightforward method. The commonly used solvents are N,N-dimethylformamide (DMF), dichloroethane (DCE) and N-methyl-2-pyrrolidone (NMP). Low concentration of CNTs and high boiling point of these solvents are two important obstacles for fabrication of high performance TCFs. Furthermore, CNT dispersion into these organic solvents typically requires excessive sonication that can lead to considerable mechanical damage and thereby electrical degradation of the nanotubes. The maximum concentrations of SWCNTs are usually lower than 0.1 mg/mL, much lower than the requirements for industrial applications (>1 mg/mL) [1]. Solubility of SWNTs in variety of solvents is given in Table 3.1 [45]

Table 3.1 : Solubility of SWNT in a variety of organic solvents.

Solvent	Solubility (mg/L)
1,2-Dichlorobenzene	95
Chloroform	31
1-Methylnaphthalene	25
1-Bromo-2-methylnaphthalene	23
N-Methylpyrrolidinole	10
Dimethylformamide	7.2
Tetrahydrofuran	4.9
1,2-Dimethylbenzene	4.7
Pyridine	4.3
Carbon disulfide	2.6
1,3,5-trimethylbenzene	2.3

It can be clearly seen from Table 3.1 that all solvents with a solubility over 20 mg/L have some sort of electronegative end group. With the exception of chloroform, the other three chemicals contain a benzene ring. Therefore, it can be assumed that in organic solvent, pi-pi interactions are useful (but not 100% necessary) for interactions with CNTs. The electronegative groups may act as a charge barrier to prevent agglomeration [46].

Using surfactants for dispersion of CNTs is another common method due to its ability to individualize CNTs at high concentrations, and its ability to be rinsed off by washing of the film [39,47-49]. Furthermore, water-soluble surfactants can be used, leading to aqueous-based CNT dispersions. The hydrophobic end of a surfactant attaches to CNTs, while the hydrophilic end helps pull the CNTs into solvents such as water. The π -like stacking of benzene rings benefits the binding of surfactant and CNTs. The headgroup, chain length, and surfactant weight are the main factors that are found to affect the dispersion ability of the surfactant. Although many surfactants have been investigated, the most commonly used for TCF assembly are sodium dodecyl sulfate (SDS), sodium dodecyl benzene sulfonate (SDBS), sodium cholate (SC) and commercial Triton X-100 [1]. Figure 3.1 shows a schematic representation of how surfactants may adsorb onto the nanotube surface.
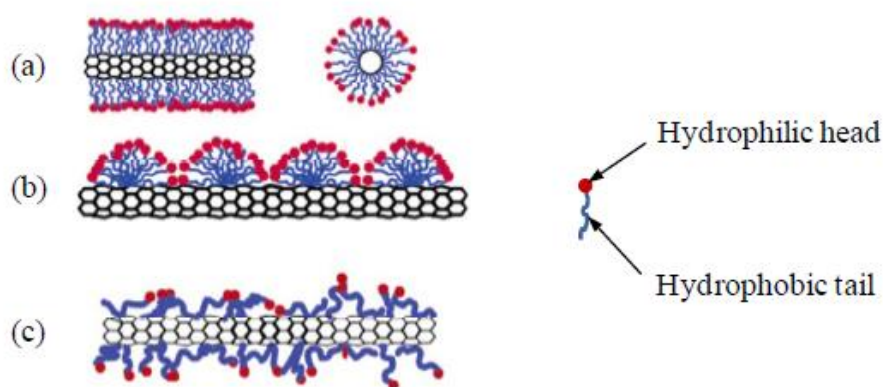
Figure 3.1 : a) Cylindrical adsorption, b) hemispherical adsorption and c) random adsorption of surfactants on SWCNT surface [49].

There are several advantages of using surfactants to disperse CNTs: (i) CNTs can be dispersed at high concentrations up to 20 mg/mL [50]. (ii) The original electrical properties of CNTs are not altered by surfactant dispersion. (iii) More importantly, water can be used as a solvent, which is cost-effective, environment-friendly and safe. However, surfactants are usually insulating, so a washing-out step is crucial to remove them after film formation [2].

Research on covalent functionalization of CNTs with different organic or inorganic functional groups started almost at the same time as the discovery of CNTs, and many reviews have been published [51,52]. CNTs are chemically treated to introduce negatively charged carboxylic groups on their surfaces, so that a stable CNT aqueous

dispersion can be obtained without any surfactant. Functionalization of CNTs is achieved by introducing defects in crystal structure, resulting degradation of electronic properties of CNTs. The number of reports on the use of covalently functionalized CNTs for the fabrication of TCFs is very limited [53,54]. Though such a dispersion can be used to make large area films, their optoelectrical performance is rather poor with a typical sheet resistivity (R_s) value about 2.5 kΩ/sq at a transparency of 86.5% [53].

3.1.2 Deposition techniques

Once a stable CNT dispersion is obtained, deposition of the tubes onto a substrate proves a significant challenge. As compared to direct CVD growth, solution-based deposition can be preferred for several reasons: (i) The low temperature process allows deposition onto arbitrary substrates. (ii) The deposition process can be easily scaled to large areas. (iii) Process does not require high vacuum, which significantly reduces the cost.

The basic concept of a solution based deposition process is to coat CNT solution homogenously onto substrate followed by evaporation of solvent without causing agglomeration. Therefore, solution/substrate interactions also need to be considered. In some cases, an additional step of removing surfactant or polymer is necessary [55].

3.1.2.1 Dip coating

Dip coating is extremely simple and cost effective deposition technique, but also potentially time consuming for fabrication of CNT-TCFs. Viscosity of SWNT solution, SWNT ink-substrate interaction, coating speed and drying conditions are the most important parameters that can easily affect the SWNT film quality.

In this method, a substrate is immersed into the CNT dispersion, as shown in Figure 3.2, and removed after a specific amount of time for coating to take place. Immersion steps can be repeated until desired thickness of the CNT-TF is obtained. A rinse after each deposition layer is required to remove impurities from the surface. Dip coating method has been utilized to fabricate SWNT thin films on various substrates for different applications [56,57].
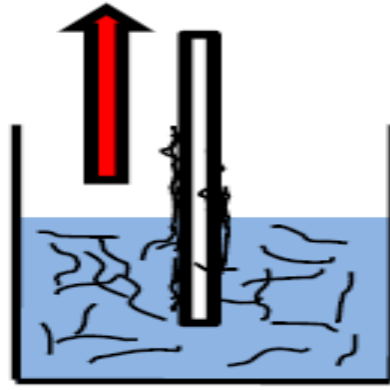
Figure 3.2 : Schematic illustration of the dip coating method [56].

3.1.2.2 Spray coating

Spray coating is another solution based deposition technique for fabrication of SWNT thin films. Spray coating is a simple, fast and low cost technique that does not require high vacuum system. Furthermore, large and flexible substrates can be coated very quickly and SWNT thin film conductivity can be tuned easily.

In this method, SWNT dispersion is sprayed onto a substrate, which is usually fixed on a stage heated to appropriate temperature for evaporation of the solvent. Spraying can be done using an air-brush pistol, or an atomizing nozzle. In both cases, a pumping or a steering unit is needed to carry the solution to the heated substrate with a constant flow rate. Many researchers have used spray coating for the deposition of SWNT networks [57-63]. Especially in fabricating large area flexible electronic devices, spray coating has obvious advantages over other techniques.

Spray coating method has many advantages over other solution based deposition methods. However, set-up properties such as stage scan speed, substrate temperature and flow rate should be optimized first in order to obtain high quality CNT-TFs.
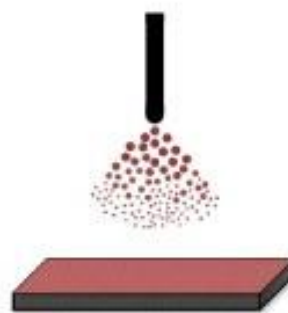
Figure 3.3 : Schematic illustration of the spray coating method [64].

3.1.2.3 Spin coating

Spin coating is another commonly used solution-based deposition technique. This method is based on placing an excess amount of solution on the substrate that is subsequently rotated at high speeds (between 2000-8000 rpm), to produce a centrifugal force that spreads the fluid uniformly over the substrate (Figure 3.4).

SWNT thin film thickness, conductivity and the optical transmittance values can be controlled by the number of coatings. High degree of dispersion of SWNTs is required for fabrication of uniform transparent SWNT thin films [65].

Dichloroethane (DCE) is commonly used to prepare SWNT dispersions for spin coating due to its volatility [66]. Surfactant assisted SWNT dispersions can spin coated on various substrates [67].

Spin coating is not suitable method for many SWNT thin film applications because it requires multiple coating cycles to make an uniform film and it can not be scaled-up.
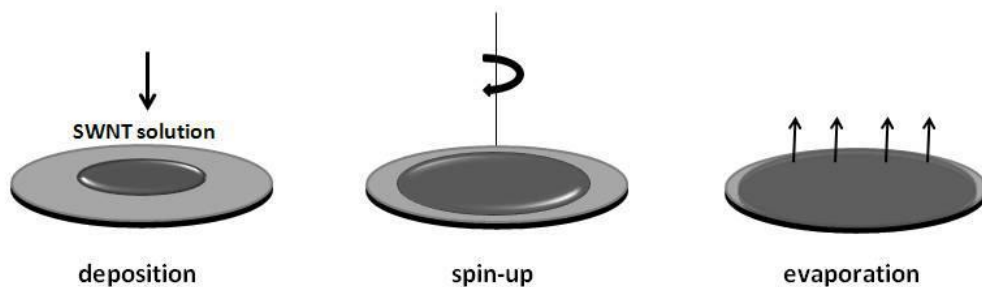
Figure 3.4 : Schematic illustration of spin coating process.

3.1.2.4 Vacuum filtration

Vacuum filtration is the most commonly used method for the fabrication of CNT thin films. The process involves a vacuum-induced flow of CNT dispersion through the mixed cellulose ester (MCE) filter membranes [68]. As the solution is filtered through the membrane, CNTs are collected forming an interconnected surface. After filtering the CNT suspension, the membrane should be washed with several milliliters of deionized water to remove the residual surfactant.

For transfer process, membrane is placed on the substrate and dried on hot plate at 70°C under compressive loading to promote adhesion. Multiple acetone baths are applied to remove MCE membranes completely from substrate surface. Film

thickness can be easily controlled by the volume of the filtered CNT solution and CNT concentration (Figure 3.5).
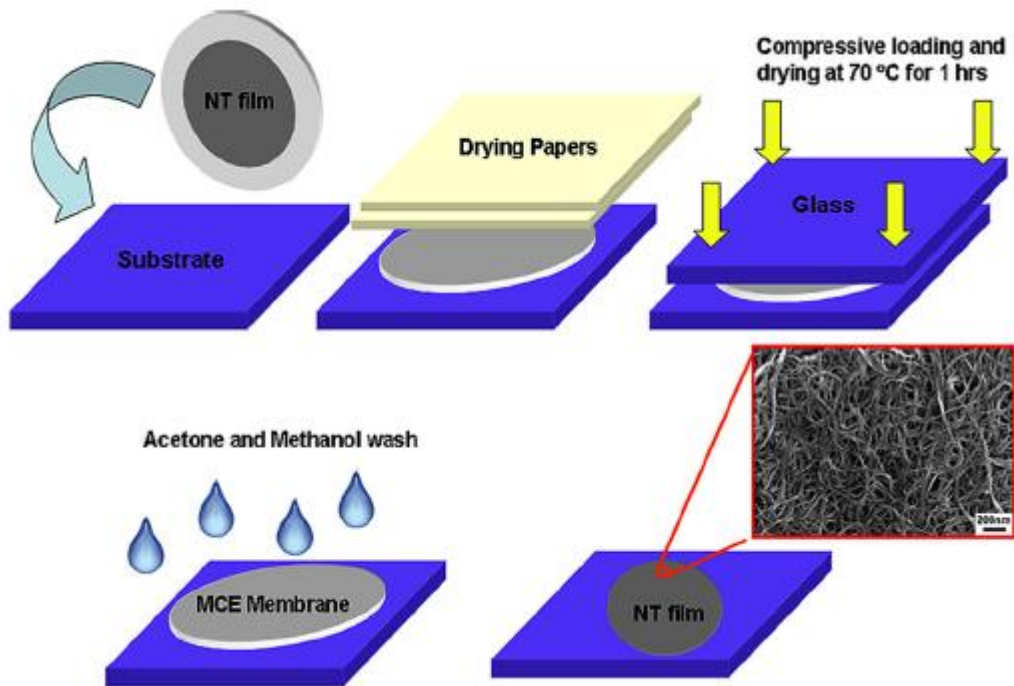
Figure 3.5 : Illustration of the SWCNT film transfer via MCE dissolution process. The process proceeds from left to right [69].

3.1.3 Modification of carbon nanotube thin films

Doping of CNT thin films is essential step for further performance improvement and modifications. This process increases the delocalized carrier density, while lowering the intertube conduction barrier [70–72] resulting in conductivity improvement for TCFs.

Covalent doping affects the intrinsic transport properties of CNTs (typically decreases the mobility), but have good stability, while non-covalent doping has a lower binding energy (less stable) but has a lower impact on charge carrier mobility [1].

For several years it was propagated that purely metallic carbon nanotube networks (CNNs) would give an optimal conductivity, but the recently availability of highly enriched material led to analyses with unexpected results. Blackburn et al. discovered that redox-doped semiconducting CNNs have higher conductivity than metal-enriched films [73]. The cause can be explained by shifting of Fermi level (EF) toward the valence band. With sufficient doping, the EF into the van Hove

25

singularities outside of the energy gap, leading to a higher density of free charge carriers in s-SWNTs than in m-SWNTs. Additionally, the intertube barrier is lowered more efficiently for junctions of s-SWNTs. A possible drawback of the p-type doping is the simultaneous increase in the work function [74]. It also reduces the stability in regard to the level of doping.

The p-type dopants for CNTs include acids such as HNO_3, gases such as O_2, NO_2, and Br_2, molecules such as $SOCl_2$ and F4TCNQ, polymers, and transition metals. The doping process is extremely simple and usually consists of dipping the CNT thin films on substrates into the dopant solutions for a certain amount of time. Resistance measurement before and after the chemical treatment reveals a dramatic increase in conductivity.

3.2 Evaluation of CNT-TCFs

Figure of merit (FoM) is required for evaluation of the quality of fabricated TCFs. Several FoMs are used to compare the electrical and optical performance of TCFs [75,76]. The primary FoMs used to evaluate SWNT networks as transparent conductors are sheet resistance, R_s and optical transmittance, T at 550 nm. Prior to presenting the factors influencing thin film properties, these primary figures of merit will be discussed in the following section.

3.2.1 Sheet resistance

The sheet resistance of SWNT networks is very important because of its contribution to the resistive power losses in organic devices. R_s is used to characterize the two-dimensional electrical properties of the conductor. This property assumes negligible current flow in the direction perpendicular to the plane of the electrical conductor, thereby only describing lateral conduction within the film. It is given in terms of Ω/sq, and is defined as,

$$R_s = R\frac{W}{L} \tag{3.1}$$

Therefore, R_s can be simply understood to give the resistance, R, between two contacts of width, W, at a length, L, apart. Due to the percolating nature of SWNT networks, R_s is expected to vary inversely with film surface density [77]. Since

surface density is directly proportional to film thickness (t), R_s should also scale with the inverse of film thickness. An example of this relationship is shown in Figure 3.6. A clear inverse relationship can be seen between R_s and the film thickness, as R_s approaches a saturation level. As the film thickness increases, more conducting pathways are created.
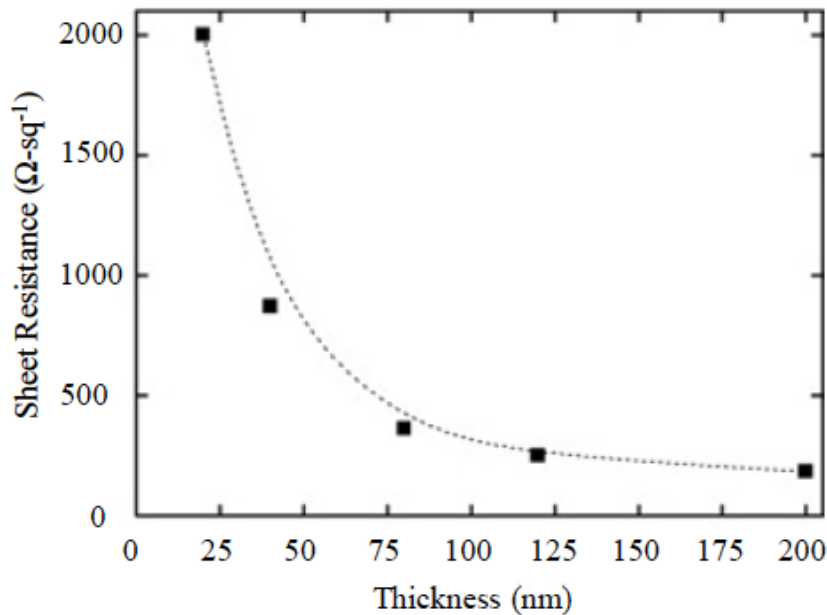
Figure 3.6 : R_s as a function of SWNT film thickness [78].

3.2.2 Optical transmittance

Typically when the optoelectronic properties of transparent electrodes are presented in the literature, the optical transmittance near the visible spectrum is given [79]. Only wavelengths near the visible spectrum are shown for electrodes employed in organic electronics because OLEDs emit colors visible in this range, while the optimal absorption efficiency of OPVs is in the range of 400-800 nm.

Sample SWNT films of varying thickness are shown in Figure 3.7 [78]. It can be seen that the optical transmittance decreases with increasing film thickness. By convention, the transmittance at 520 or 550 nm is given as a representative value of the overall transmittance in the visible spectrum due in large part to the relative optical consistency of transparent conductors used as electrodes for organic devices (e.g. Figure 3.7) [80]. Therefore, optical transmittance at 550 (or 520) nm can be seen as a useful gauge of the transmission losses due to absorption by the electrode.
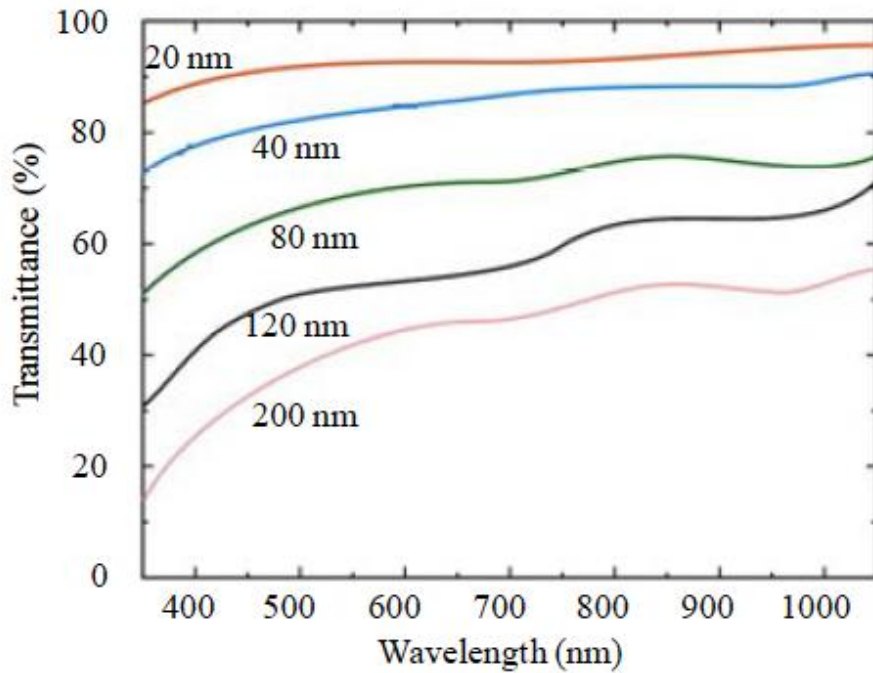
Figure 3.7 : Optical transmittance of SWNT films of several thicknesses [78].

As seen in Figure 3.8, optical losses increase with increasing film thickness due to lower film transmittance while electrical losses decrease with a similar increase in thickness. Therefore, a tradeoff must be achieved between optical and electrical losses in SWNT films.
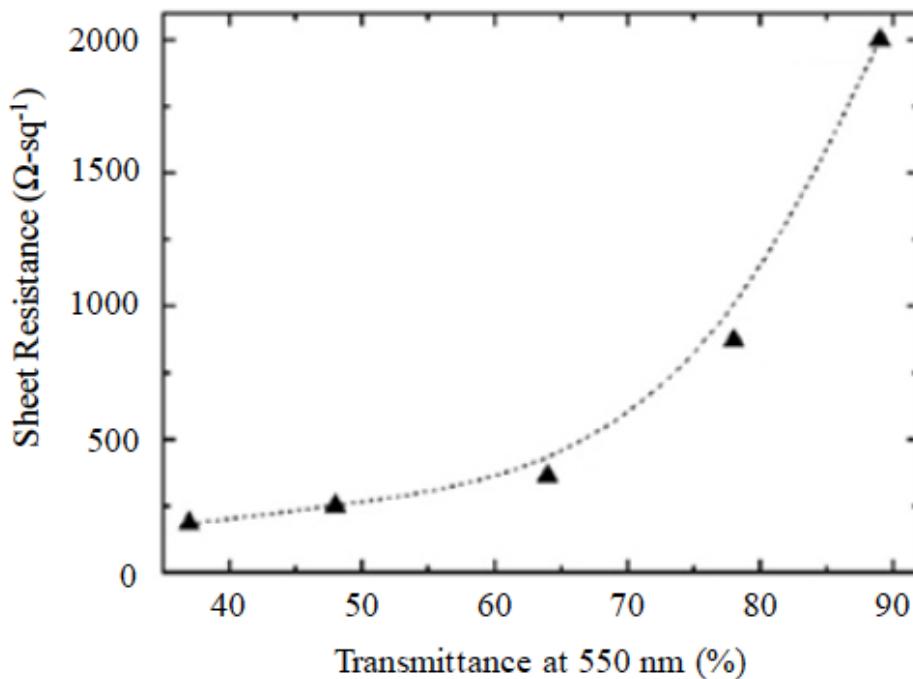
Figure 3.8 : Correlation between transparency and R_s. Film transparency represented by transmittance at 520 nm [40].

Shown in Figure 3.8 is a plot of the corresponding relationship and expected competing performance goals. Since, a decrease in R_s is most often accompanied with a decrease in transmittance, they are most often combined when presented. In this regard, R_s is often quoted with a given transmittance at 550 nm. Since 80% transmittance at 550 nm is often viewed as a standard benchmark transmission that SWNTs transparent electrodes must meet or exceed to be a viable replacement for ITO, R_s is often presented with transmittance $\geq$ 80% [81,82]. State of the art optoelectronic values of pristine SWNT films include R_s of 186 Ω/sq and 129 Ω/sq with transmittances at 550 nm of 86% [82] and 80% [83] respectively. It must be noted that these state of the art values represent by far some of the best optoelectronic values seen in the literature. Typical R_s values with transmittances at 550 nm of 80-85% are in the range of 250 Ω/sq-400 Ω/sq [74,84,85], with many R_s values presented on the kΩ/sq range for a similar transmittance [56,86].

3.3 Factors Influencing Thin Film Properties

The conductivity of CNT-TCFs produced by wet processes depends on the formation of conductive networks. Basically, the electrical conductivity of individualized nanotubes must be high enough to achieve a low R_s of thin films and the lattice perfection of CNTs is the key element. As a result, covalently functionalized CNTs are seldom used for a CNT-TCF assembly [1].

Furthermore, CNT purity is another critical factor in determining film conductivity. The presence of amorphous or sp^3 bonded carbon and surfactants will decrease the conductivity of resulting TCFs. Typically, films with higher Raman G/D band intensity ratios exhibit higher conductivity [87]. This means that fabrication, purification and post treatment to remove surfactants are critical factors for obtaining highly conductive TCFs.

In addition, the anisotropic conductivity of individual nanotubes results in a high contact resistance between connected CNTs. As a result, factors that can influence the contact resistance between CNTs are also key factors that influence the film conductivity.

The main factors influencing the performance of CNT-TCFs include the type of nanotubes, mean tube/bundle length and size (diameter), and the formation of

networks (network density and film thickness). As to the effect of CNT type shown in Figure 3.8 (a) and (b), SWCNT-TCFs have the best performance compared with those assembled from MWCNTs and DWCNTs. And TCFs fabricated with SWCNTs that are produced by arc discharge show obvious superiority than that by laser ablation and CVD with high-pressure carbon monoxide (HiPCO). One explanation is that the former can form a better networks than the latter two types of tubes.

Longer CNT bundles will limit the number of CNT junctions per unit area of film and result in a higher conductivity of the network (Figure 3.8 (c)) [88]. Smaller bundles lead to higher conductivity with the same transparency (Figure 3.8 (d)) [89] due to the decrease of non-current carrying tubes in the middle of CNT bundles. In addition, orientation of the bundles can affect the efficiency of the conductive network. High contact angle X-type contacts are found to produce larger contact resistance than low contact angle Y-type contacts [90].
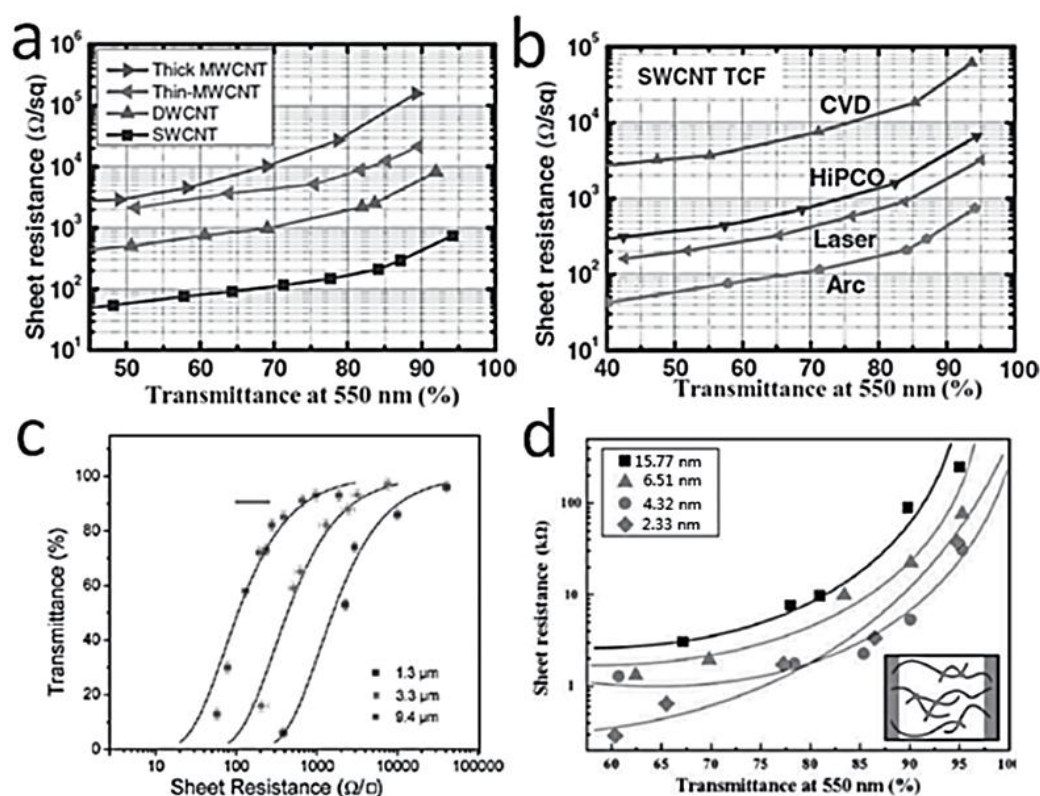
Figure 3.9 : Factors influencing the performance of CNT-TCFs a) CNT types [91] b) Synthesis methods of SWCNTs [92] c) Mean bundle lengths [88] d) Mean bundle diameters [89].

4. EXPERIMENTAL STUDIES

4.1 Synthesis and Purification of SWCNTs

SWNTs used in this study were synthesized in a fluidized bed CVD system method in Material Production and Preparation Laboratory of Energy Institute in Istanbul Technical University. The system consists of 3 cm diameter quartz reactor placed in a vertical furnace. The precursor was loaded in the middle of the reactor on a nanoporous silica disc. CNT production was held on the 5 to 10 cm length region around the quartz disc of the reactor on the quartz reactor. To fluidize the bed a certain flow rate of gas was necessary for a given substrate catalyst mixture. For this purpose argon was used as carrier and inert gas and acetylene was used as carbon source. The gas was fed to the system through the bottom of the reactor and it leaves the system from the top. Schematic view of CNT production is given in Figure 4.1.

high surface area MgO powder (A=100 $m^2 \cdot g^{-1}$)

impregnation in a $Fe(NO_3)_3$ ethanol solution

drying

heating
$\Rightarrow$ formation of Fe_2O_3 cluster

pyrolysis of C_2H_2 in Ar atmosphere

$\Rightarrow$ Nanotubes grow on powder surface
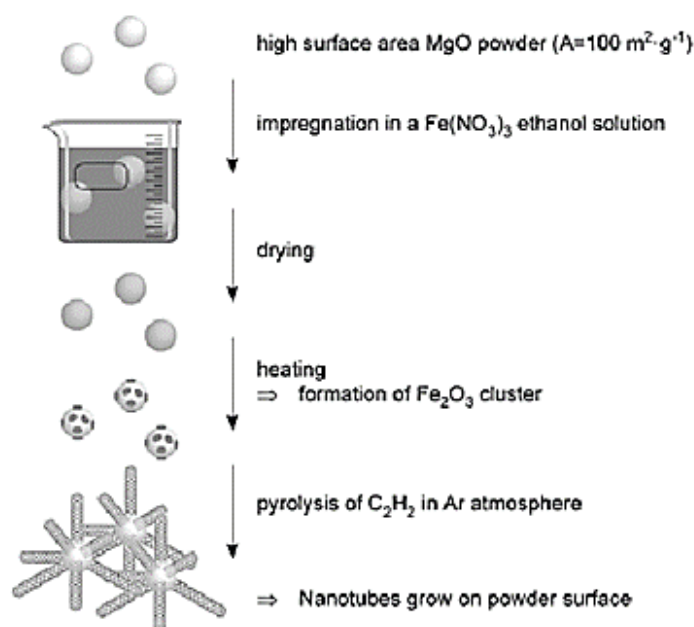
Figure 4.1 : The precursor powder preparation and CNT growth on powder grains.

High purity Ar gas was purged to obtain an inert atmosphere and then the system was heated up to 800 °C. SWCNTs were grown on metal catalyst (Fe-MgO) with

acetylene (C_2H_2) as carbon precursor for 30 minutes. After synthesis, SWCNTs were purified by nitric acid treatment of 6M HNO_3 for 3 hours at 120 °C to remove metal catalysts.

4.2 Fabrication of CNT Thin Films

In this study, spray coating method is utilized for fabrication of CNT thin films. Sonication, centrifugation, post-deposition acid treatments have also been applied in order to improve the film quality and optoelectronic properties of films.

4.2.1 Substrate cleaning

Glass substrates used in this study were cleaned by sonication in subsequent deionized (DI) water, acetone, isopropyl alcohol baths for 15 minutes each.

4.2.2 Dispersion of CNTs

Dispersion of CNTs is quite important step for achievement of homogeneous thin films. Two different dispersion routes were selected in order to investigate the effect of dispersion media.

4.2.2.1 Dispersion of CNTs in neat solvent

Dispersions of CNTs in N-Methyl-2-pyrrolidone (NMP) were prepared with concentration of 0.2 mg SWNT/ 1 mL NMP. This mixture was sonicated for 1 hour at 225 W using a Cole-Parmer Ultrasonic cup-horn sonicator. The sonicator was operated at 10% with an approximate sonication power of 22.5 Watts. For purification, this dispersion was then centrifuged for 30 minutes at 8000 rpm. The solution was subsequently and carefully decanted such that only the top 90% of the sample was removed for further processing.

4.2.2.2 Surfactant assisted dispersion of CNTs

For surfactant assisted CNT dispersion, sodium dodecyl sulfate (SDS) was disolved in deionized water with a weight ratio of 0.5%. SWNTs with a concentration of 0.05 wt % were added and the solution was sonicated for 15 minutes at 225 W using a Cole-Parmer Ultrasonic cup-horn sonicator. The sonicator was operated at 20% with an approximate sonication power of 22.5 Watts. For purification, this dispersion was then centrifuged for 30 minutes at 8000 rpm. The solution was subsequently and

carefully decanted such that only the top 90% of the sample was removed for further processing.

4.2.3 Deposition process

4.2.3.1 Spray coating

Spray coating is as a simple and cost effective thin film deposition technique and also suitable for large area applications. In this technique, substrates were placed onto a heater on which the temperature was maintained at 200°C for neat solvent, and at 100°C for surfactant assisted coatings. The supernatant of CNT solution was loaded into a commercial airbrush, and repeatedly sprayed onto a glass substrate until the desired transmittances were reached. Heat was applied in order to avoid fine droplets. SWCNT solutions were spray coated onto 1x1 cm^2 glass substrates. Spraying conditions were optimized to reach the best film performance. The distance between the nozzle and the substrate was 10 cm.

4.2.4 Post-deposition acid treatment

Post-deposition acid treatments were utilized in order to improve electronic properties of CNT thin films. CNT films were immersed in 13 M HNO_3 for 30 minutes and then were carefully dried with air flow.

For surfactant assisted coatings, CNT thn films were firstly immersed in 4 M HNO_3 overnight for removal of surfactant and then films were soaked in 13 M HNO_3 as described above to improve electronic properties.

4.3 Characterization of CNT Thin Films

4.3.1 Scanning electron microscope

Homogeneity and morphology of the fabricated SWCNT thin films were analysed by field emission scanning electron microscopy (FEI-Quanta FEG 250). The operating voltage was between 10 and 15 keV.

4.3.2 Optical transmittance measurements

Transmittance measurements of the SWCNT thin films were performed at room temperature using a UV-Vis spectrometer (T80 UV-Vis) within the range of 300 -

1100 nm wavelengths. A clear bare glass slide was used for the baseline correction.

4.3.3 Sheet resistance measurements

Sheet resistance measurements of SWNT thin films were performed using a four probe measurement set-up. Keithley 2400 sourcemeter was used to apply current and measure the resulting potential drop. Voltage drop was measured with applied currents between 5 µA- 50 µA for 15 points and converted to a sheet resistance using

$$R_s = \frac{\pi}{\ln 2} \frac{V}{I} \cong 4.53 \frac{V}{I} \qquad (4.1)$$

5. RESULTS AND DISCUSSIONS

5.1 Synthesis of SWNTs

CNT production generally requires existence of a catalyst. The selection of a proper metallic catalyst may affect the morphology amount of the synthesized product, the quality of the product. In this study, the transition metal of iron (Fe) impregnated on MgO powder substrate with weight ratio of 5:100 were used as catalysts. SWCNTs were synthesized by catalytic chemical vapor deposition of acetylene (C_2H_2) at 800 °C for 30 minutes. Thermogravimetric analysis (TGA), Raman spectroscopy and transmission electron microscope (TEM) measurements were used for CNT characterization.

TEM images of the synthesized material is given in Figure 5.1. It is evident that the structures synthesized by chemical vapour deposition method are CNTs. The CNTs have diameters between 1.5-5 nm and also are transparent. One possible explanation for the dark parts in both two figures is a result of the impurities within the structures.
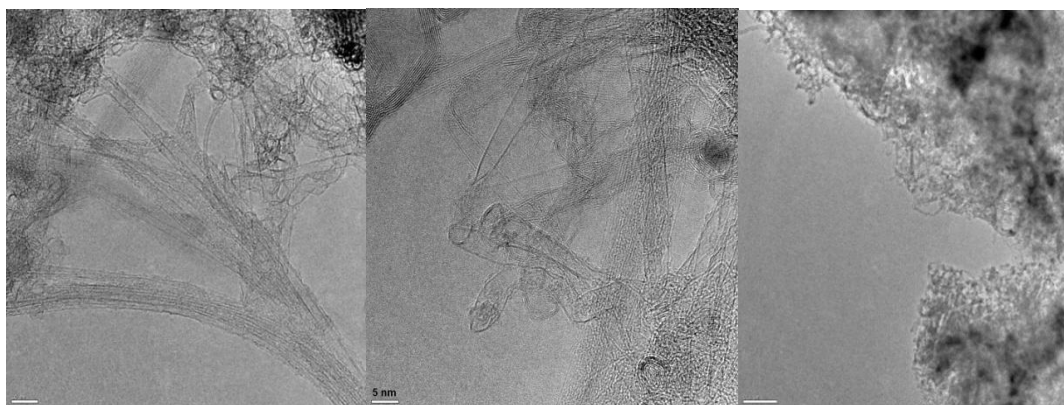
Figure 5.1 : TEM images of CNTs synthesized at 800°C.

Figure 5.2 shows Raman spectrum for carbon deposits excited by 633 nm laser. The Raman spectra show the characteristic peaks at 1300 (D band) and 1580 cm^{-1} (G band) for SWCNTs grown on the catalyst. The G and D bands correspond to the degree of graphitization and the defects in CNT structure, respectively.

In Raman spectra, the ratio of D and G band intensities (I_D/I_G) express the quality of CNTs. The lower the ratio in the spectra refers to the lower content of amorphous carbon and defect formation in the structure. The average ratio of D and G bands of SWCNTs produced on Fe catalyst was around 0,2. The intense and narrow shaped radial breathing mode (RBM) peaks of sample demonstrate that the tube diameter is below 2 nm. The mean diameter of SWCNTs can be calculated using RBM frequency unit of cm^{-1} as,

$$\omega = \frac{A}{d} + B \qquad (5.1)$$

where, A and B are constants (A=234 cm^{-1} and B=10 cm^{-1}) and d (nm) is the diameter of SWCNT. The mean diameter of the synthesized SWCNTs was calculated as 1.18 nm.
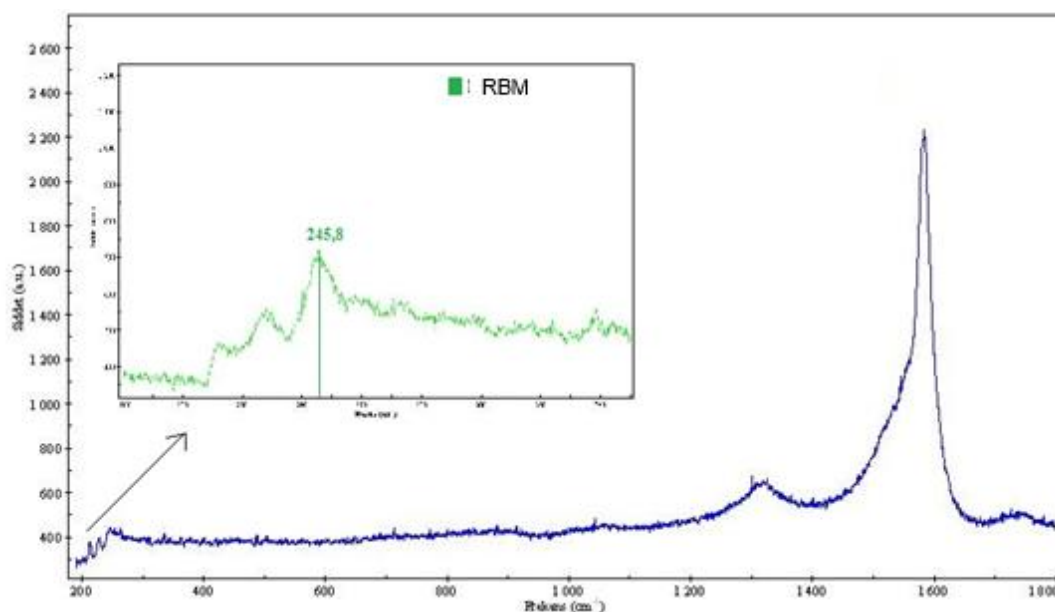
Figure 5.2 : Raman spectra of SWCNTs.

Thermogravimetric (TG) analysis is used to characterize the total carbon loading and determine the residual metallic catalyst. The amorphous carbon is completely oxidized at temperatures below 350°C and graphite burns above 750°C. The oxidation temperatures of the CNTs depend on the nanotube type and SWCNTs is generally oxidized at the temperatures above 400°C. In this study, the TG analysis of synthesized SWCNTs was conducted in air atmosphere with a ramp of 5 °C/min between 25 and 800 °C. The yield was defined as the relative weight loss due to the

oxidation of the carbon and the result of this analysis is shown in Figure 5.3. As shown in this figure, carbon nanotube sample has high metal content (about 74%). Moreover, Derivative Thermogravimetric Analysis (DTG) of the sample was accomplished and the result is also shown in Figure 5.3. Since the derivative curves directly reflect the variation in the weight as a function of temperature by occurrence of thermal events (such as the onset of burning), the discussion will focus on these. It can be seen that maximum weight loss of CNTs was occurred at 590°C (DTGmax). Especially, it is observed that DTG curve of the sample has only one peak which belongs to SWCNTs. This is the also evidence of low amorphous carbon content of the sample. Similar situation is reported on the other studies in literature and oxidation of amorphous carbon below 400°C is mentioned.
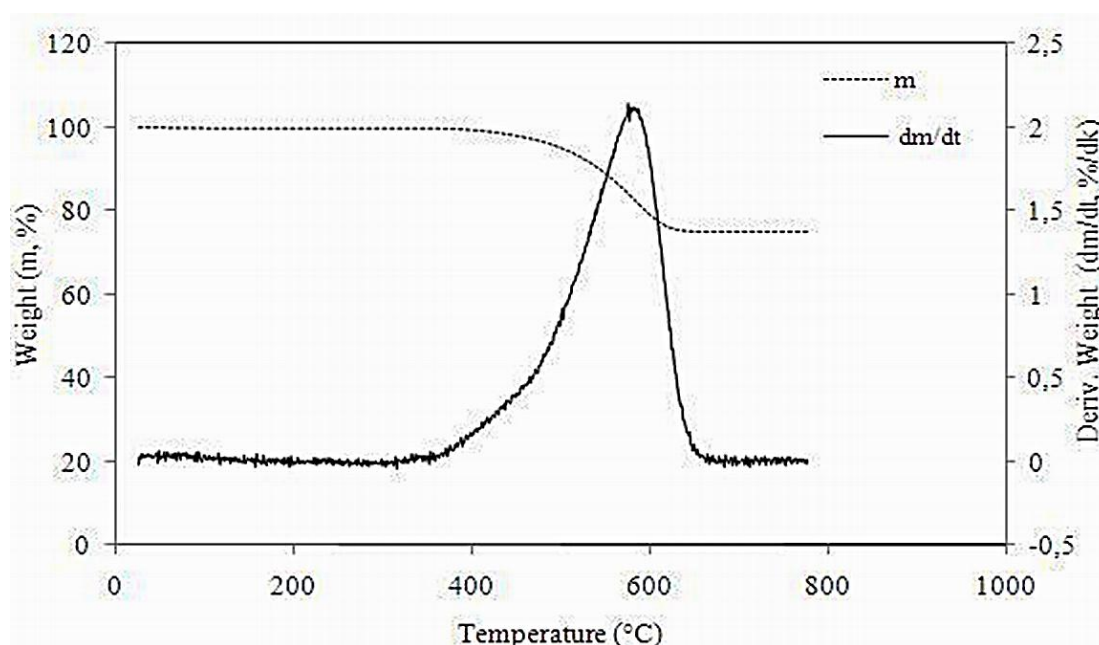
Figure 5.3 : TG and DTH curves of SWCNT synthesized at 800°C.

TG analysis of the purified SWCNTs by 6 M HNO3 for 3 h at 120 °C was performed in air atmosphere with a ramp of 5 °C/min between 25 and 800 °C. Purification yield is calculated by,

$$\text{Purification yield} = \frac{w_o - w_t}{w_o} \times 100 \tag{5.2}$$

Purification yield (%) where w_o is the metal content of as-grown SWCNT (%) and w_t is the metal content of purified SWCNT (%). The sample purified by HNO3

demonstrated a residual weight of nearly 1.19% belonging to catalyst particles which suggested efficient removal of metallic catalyst (Figure 5.4) and 98.39% purity level.
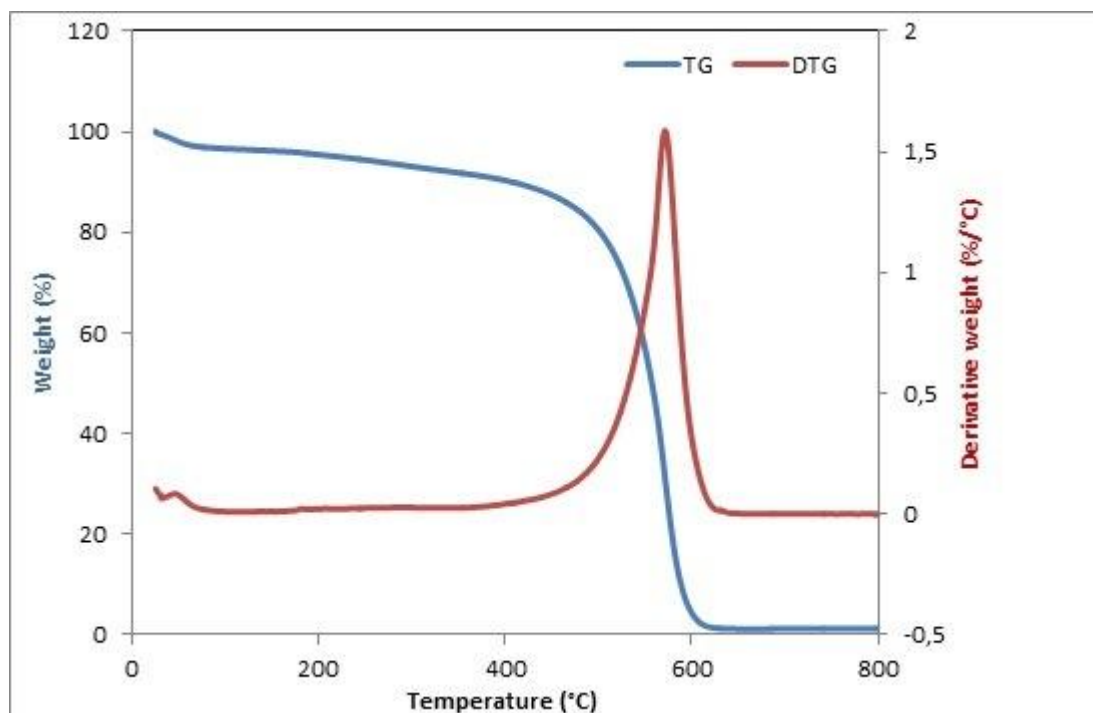
Figure 5.4 : TG and DTG curves of SWCNTs purified by HNO₃.

5.2 Fabrication of CNT Thin Films

This part discusses the dispersion, deposition and characterization of SWCNT thin films. Effects of sonication time, density of SWNT films, dispersing media, CNT type and post-deposition acid treatments were investigated.

Two different sonication durations were applied in order to find the optimum sonication time for neat solvent dispersions. After determination of optimum sonication time, obtained electronic properties of SWNT thin films were used as reference for investigation of different effects.

Surfactant assisted SWNT dispersions were prepared and resulting thin film properties were compared with reference thin films.

To explore the effect of CNT type on performance of films, Tuball SWNTs were purchased from OCSiAl company and results were compared with reference thin films fabricated by CVD-SWNTs produced in our laboratory. Moreover, SWCNT thin films were doped with nitric acid in order to improve the electrical conductivities of the thin films.

5.2.1 Effect of density

Optoelectronic properties of SWNT thin films can be tuned by varying the density of the films. In order to investigate the effect of density, SWNT solution with a concentration of 0.25 mg SWNT/ mL NMP was repeatedly spray coated on glass substrates until films with three different transmittance values TCF1 (T=60%), TCF2 (T=67%), and TCF3 (T=77%) were obtained.
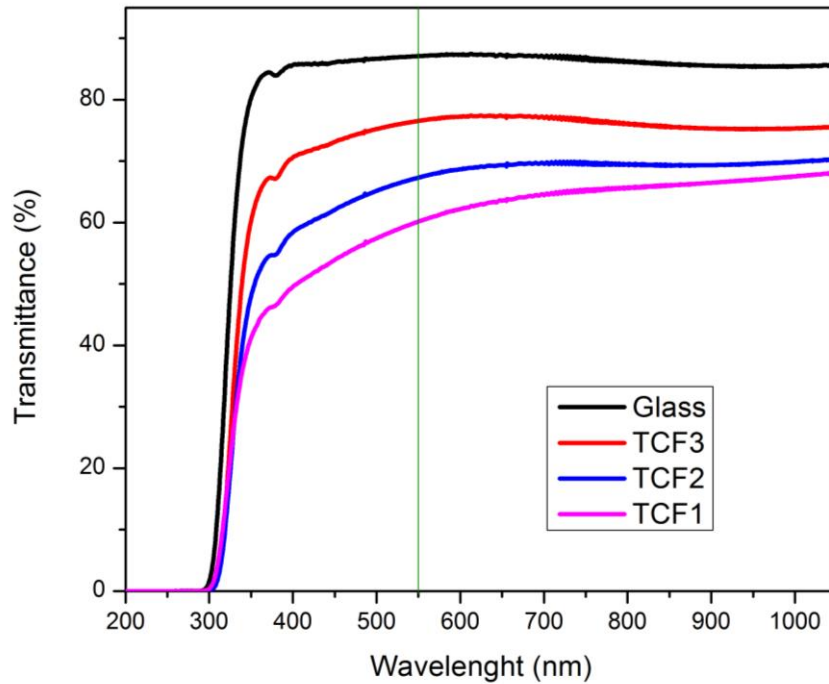
Figure 5.5 : Transmittance of the SWNT films prepared with different SWNT solution volumes.

Figure 5.5 shows the optical transmittance versus wavelength data for the films prepared with different SWNT solution volumes. The plot proves the influence of film density on the film transmittance and as expected, optical transmittance decreases with the film density.
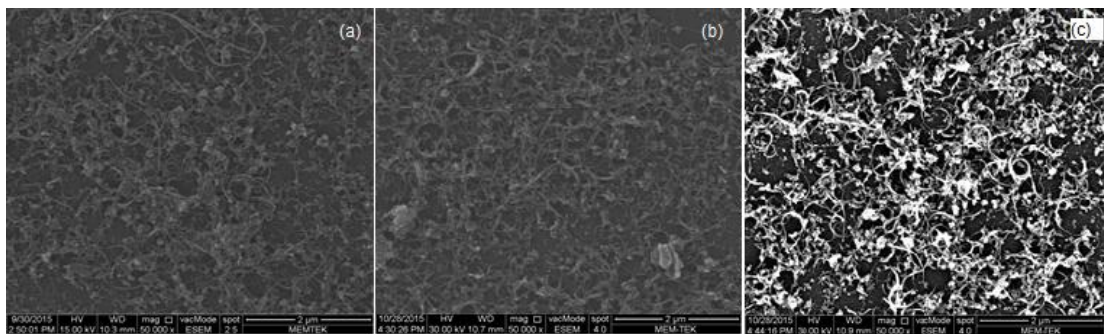
Figure 5.6 : SEM micrographs of (a) TCF1 (b) TCF2 and (c) TCF3.

Figure 5.6 shows the SEM images of SWNT thin films prepared with different SWNT solution volumes. It can be clearly seen that SWNT networks coted on glass substrates are homogenuous.

Figure 5.7 shows the correlation between the sheet resistance and transmittance of SWNT films at a wavelength of 550 nm. Transmittance decreases with the film density. However, increasing SWNT density decreases the sheet resistance of SWNT thin films due to an increase in the number of conducting pathways along the network.
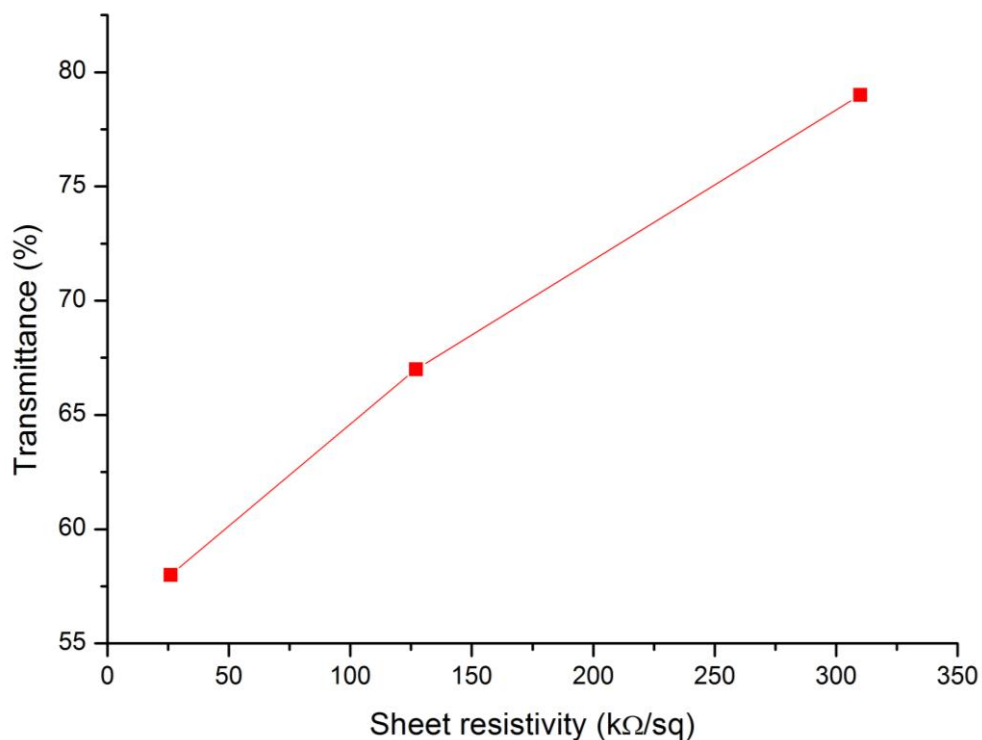
Figure 5.7 : Sheet resistance vs. optical transmittance plot for SWNT thin films.

5.2.2 Effect of sonication time

Due to the agglomeration tendency of CNTs, sonication process is quite important parameter to obtain homogeneous SWCNT dispersions. Dispersions of SWNTs in NMP were sonicated for 60 and 120 min using cup-horn sonicator operated at 10% with an approximate sonication power of 22.5 Watts.

Figure 5.8 shows the SEM micrographs of SWNT thin films fabricated by dispersions sonicated for 120 min. It can be clearly seen that CNT networks coted on glass substrates are homogenuous and only small amount of bundles can be observed.
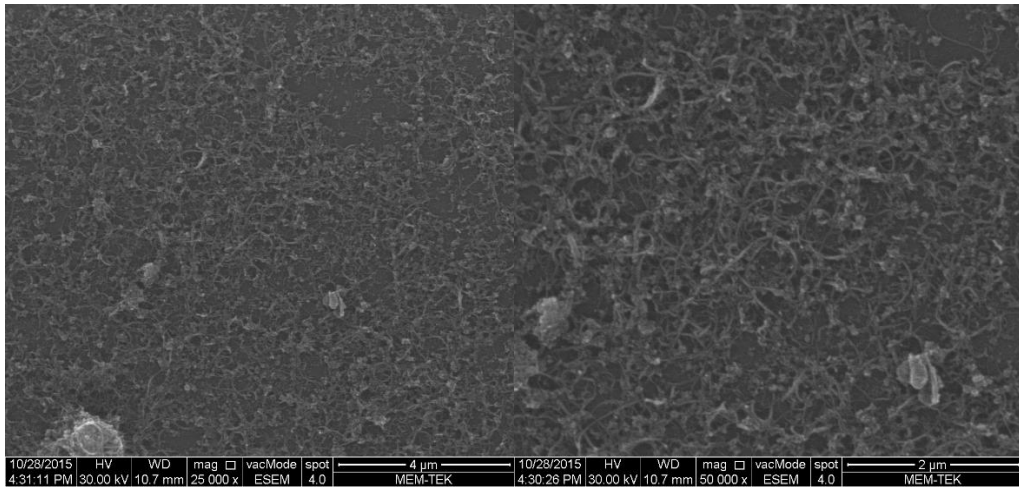
Figure 5.8 : SEM micrographs of the SWCNT thin films prepared by 120 min sonicated mixtures.

In order to obtain the optimum sonication time two dispersions were coated on glass substrates with three different transparencies and sheet resistivities were compared in Figure 5.9.
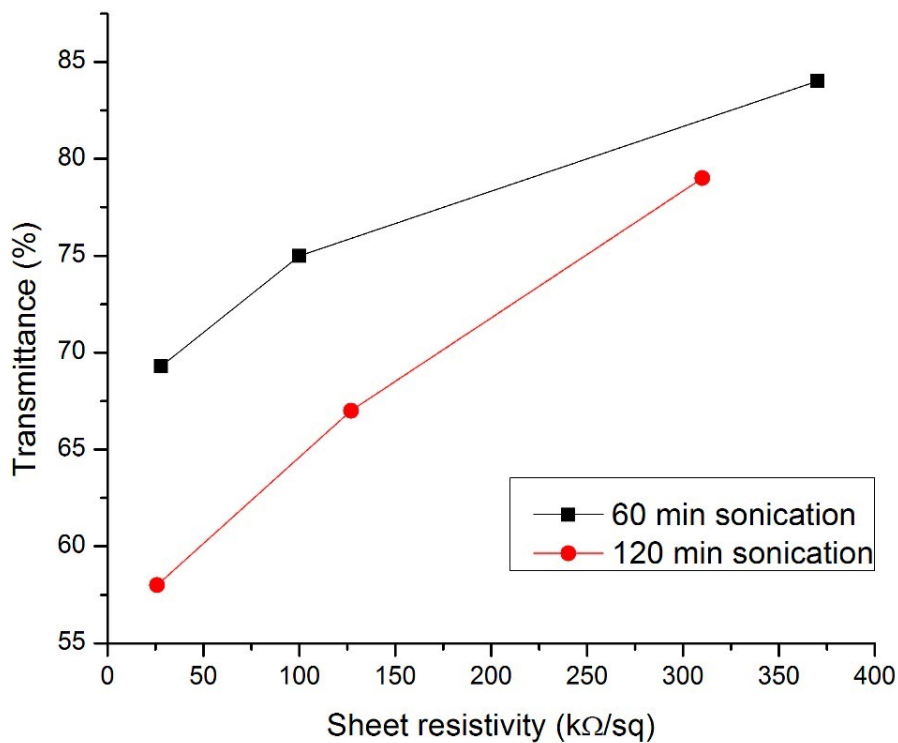
Figure 5.9 : Sheet resistance vs. optical transmittance plot of SWCNT thin films fabricated with two different sonication durations.

The data points of each set correspond to SWNT thin films with different densities. The plot proves that increasing film density improves conductivity of films due to the increase in number of conducting pathways along the network. However, optical

transmittance decreases with film density as excepted. It also can be seen that 60 min sonicated SWNT dispersions show better optoelectronic performance than 120 min sonicated dispersions, almost identical sheet resistivities were obtained at higher transparencies. Shorter sonication time introduces fewer defects to crystal structure of SWNTs resulting better electronic properties and lower sheet resistivities.

5.2.3 Effect of dispersion media

Sodium dodecyl sulfate (SDS) is the most commonly used surfactant for dispersing CNTs in aqueous media. Spray-coatable aqueous dispersions of SWCNTs were prepared, and the performance of the resultant films was compared with surfactant-free reference films prepared by spray deposition from NMP.

Low-toxicity water-surfactant mixtures are greatly preferred for large-scale manufacturing, and were consequently chosen for preparing the spray-coated films used here. The use of dispersants has the additional advantage of allowing higher SWCNT loadings to be obtained in the SWCNT solutions, thereby reducing solvent usage and sonication time, although effective post-deposition treatments are required to eliminate the surfactants.
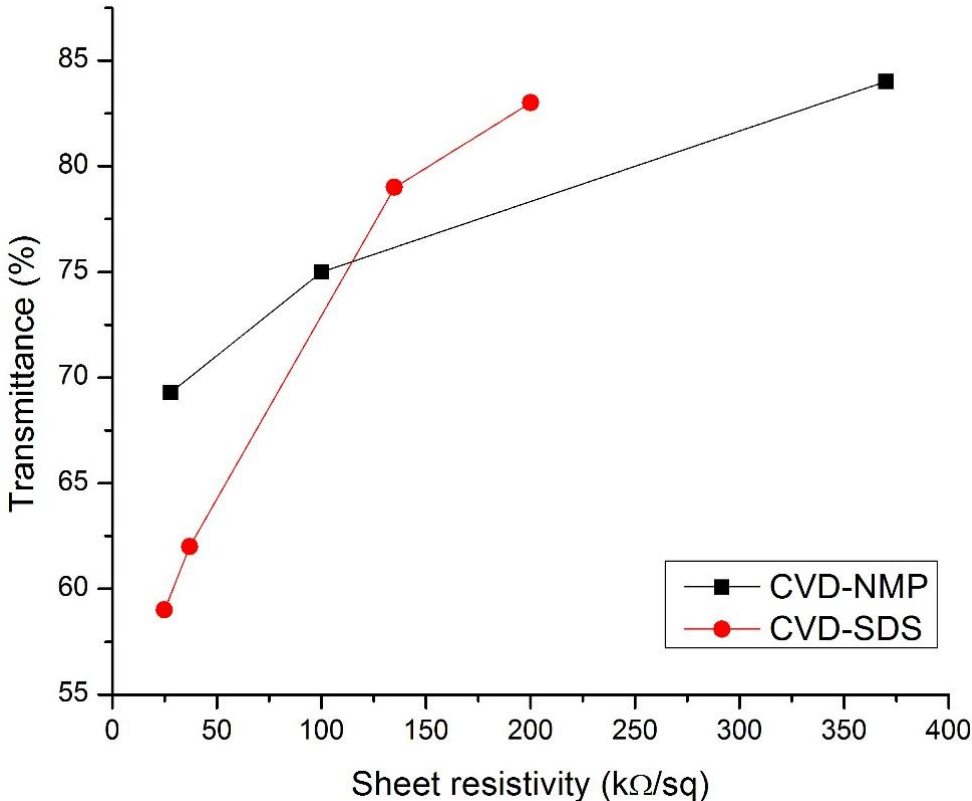
Figure 5.10 : Sheet resistance vs. optical transmittance plot of SWCNT thin films fabricated with neat solvent and surfactant assisted dispersions.

Figure 5.10 summarizes the film performances with a sheet resistance vs. optical transmittance (at 550 nm) plot. The data points of each set correspond to SWNT thin films with different densities.

SWNT thin films fabricated by surfactant assisted dispersions have shown a better performance compared to neat-solvent dispersions. Measured optical transmittance values were similar; however, their sheet resistance values were found to be different.

All of the SWCNT films were subjected to nitric acid treatments for oxidatively doping of SWCNTs and removal of surfactants and other organic contaminants.

5.2.4 Effect of CNT type

In order to investigate the effect of CNT type on performance of thin films, Tuball SWNTs were purchased from OCSiAl company and results were compared with reference thin films fabricated by CVD-SWNTs produced in our laboratory. As-prepared Tuball contains 75% and more of SWCNTs and it was used after purification with 3M HNO_3 for 1 hour in this study.

Figure 5.11 : Sheet resistance vs. optical transmittance plot of SWCNT thin films fabricated with CVD and Tuball SWNTs.

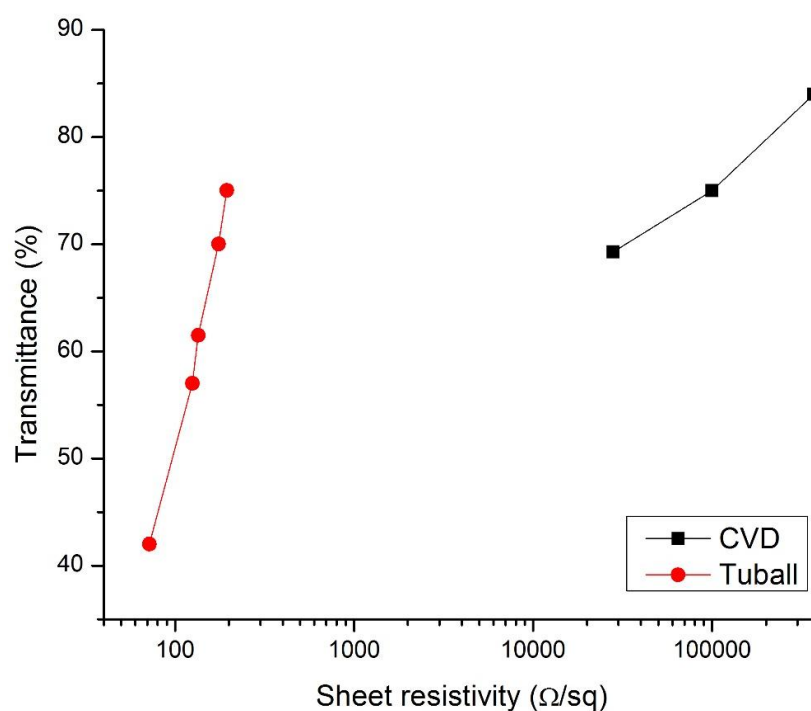Figure 5.11 summarizes the film performances with a sheet resistance vs. optical transmittance (at 550 nm) plot. The data points of each set correspond to SWNT thin

films with different densities. It can be clearly seen from the plot that thin films fabricated by Tuball SWNTs show superior performance than CVD-SWNTs synthesized in our laboratory. These results could be attributed to better crystal structure of Tuball CNTs (I_G/I_D ratio over 70) and longer tube lengths which are very important parameters for CNT networks.

5.2.5 Effect of post-deposition treatments

Doping of CNT thin films is essential step for further performance improvement and modifications. This process increases the delocalized carrier density, while lowering the intertube conduction barrier resulting in conductivity improvement for TCFs.

In order to improve the conductivity, SWNT thin films were immersed in an acid (HNO_3) bath for 30 min. It is found that sheet resistance of the SWNT thin films can be decreased by a factor of 5 after these treatments. It can be seen from Figure 5.12 that the sheet resistance decreases by a factor of 2-4 after the HNO_3 treatment.
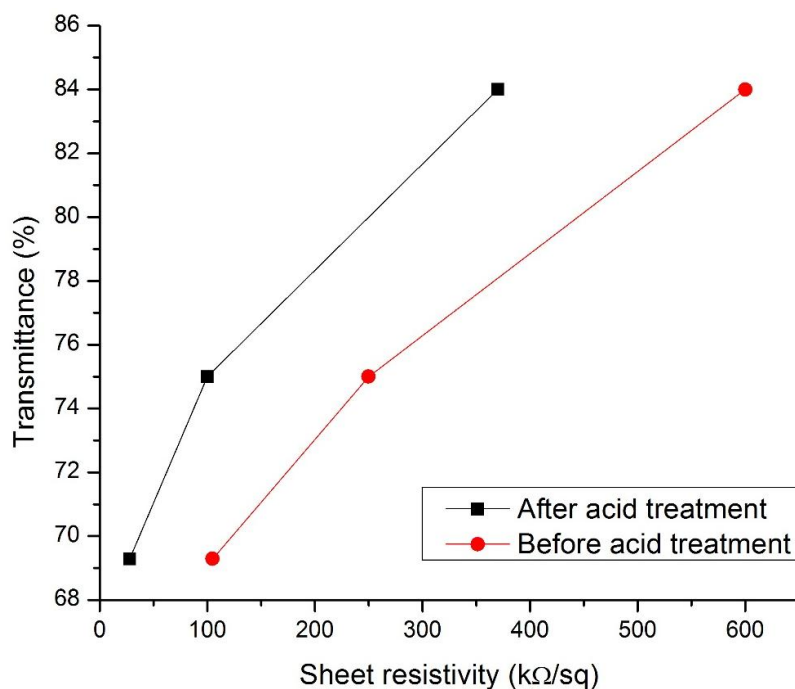
Figure 5.12 : Sheet resistance vs. optical transmittance plot of SWCNT thin films before and after acid treatments.

Optical transmittance values of the films were not affected by those treatments. These results are in agreement with the literature.

The enhancement in electrical conductivity of the films could be attributed to the increased charge carriers due the p-type doping effect.

6. CONCLUSIONS AND RECOMMENDATIONS

In this study, spray coating method was utilized for fabrication of SWNT thin films. The effects of sonication time, dispersion media, CNT type and post-deposition acid treatments were investigated on the thin film fabrication and performance. Important findings of this study are as follows:

6.1 Concluding Remarks

1. SWCNTs were synthesized by chemical vapor deposition of acetylene on Fe/MgO catalyst at 800°C and purified by 6M HNO_3 at 98.39 % purity level.

2. SWCNT thin films were fabricated by spray coating method and effect of different parameters (sonication time, dispersion media, CNT type, post-deposition acid treatments etc.) was investigated.

3. Sonication duration is one of the most important parameters for preparation of homogeneous SWCNT solutions. Two different sonication durations were utilized. 60 min sonicated SWNT dispersions show better optoelectronic performance than 120 min sonicated dispersions, almost identical sheet resistivities were obtained at higher transparencies. The lowest sheet resistivity values for fabricated thin films are 28 kΩ/sq (T=70) and 26 kΩ/sq (T=58) for 60 min and 120 min respectively.

4. Density of SWCNT on the glass substrates directly affects sheet resistance and optical transmittance values of SWCNT thin films. Increasing SWNT density decreases the sheet resistance of SWNT thin films due to an increase in the number of conducting pathways along the network.

5. All of the fabricated films are found to be mechanically robust, with no tendency to delaminate from the underlying substrate during handling.

6. Dispersion media is another crucial factor for solution based SWCNT thin films. SWNT thin films fabricated by surfactant assisted dispersions have shown better performance compared to neat-solvent dispersions. Measured optical transmittance values were similar; however, their sheet resistance

values were found to be different

7. CNT type is another important parameter for fabrication of conductive thin films. Tuball SWNTs show superior performance than CVD-SWNTs synthesized in our laboratory. These results could be attributed to better crystal structure of Tuball CNTs (I_G/I_D ratio over 70) and longer tube lengths that are very important parameters for CNT networks. The difference between sheet resistivity values is nearly 3 orders of magnitude, for similar transparencies.

8. Optoelectronic measurements of the fabricated SWCNT thin films revealed that post deposition acid treatments enhanced conductivities of SWCNT thin films by factors of 2-4, without affecting transparencies.

6.2 Recommendations

The research in this thesis has been conducted in order to investigate the potential performance of CVD synthesized SWNTs as transparent conductors. Spray coating method was utilized for NMP dispersed SWNT solutions and homogeneous thin films were obtained. Another solvent or surfactant assisted dispersions can be utilized to improve the stability of the SWNT dispersion and spray coating can be done using ultrasonic atomizer in order to make more homogeneous SWNT films. Spraying parameters can also be varied depending on the new SWNT dispersion.

In the further studies, different SWCNT types and deposition techniques can be examined to obtain the best optoelectronic performance.

REFERENCES

[1] **Hu, L., Hecht, D. S., Gru, G.** (2010). Carbon Nanotube Thin Films: Fabrication, Properties , and Applications. *Thin Film.*, 5790–5844.

[2] **Du, J., Pei, S., Ma, L., Cheng, H. M.** (2014). 25th Anniversary Article: Carbon Nanotube- and Graphene-Based Transparent Conductive Films for Optoelectronic Devices. *Adv. Mater.*, *26* (13), 1958–1991.

[3] **Kumar, A., and Zhou, C.** (2010). The race to replace tin-doped indium oxide: which material will win?. *ACS Nano*, *4* (1), 4-11.

[4] **Wu, J., Agrawal, M., Becerril, H. A., Bao, Z., Liu, Z., Chen, Y., Peumans, P.** (2010). Organic light-emitting diodes on solution-processed graphene transparent electrodes. *ACS Nano*, *4* (1), 43–48.

[5] **Hecht, D. S., Hu, L., Irvin, G.** (2011). Emerging Transparent Electrodes Based on Thin Films of Carbon Nanotubes, Graphene, and Metallic Nanostructures. *Adv. Mater.*, *23* (13), 1482–1513.

[6] **Hu, L., Kim, H. S., Lee, J. Y., Peumans P., Cui, Y.** (2010). Scalable coating and properties of transparent, flexible silver nanowire electrodes. *ACS Nano*, *4* (5), 2955–63.

[7] **Pierson, H. O.** (1993). *Handbook of carbon, graphite,diamond and fullerenes*. Noyes Publications.

[8] **Popov, V. N.** (2004). Carbon Nanotubes: Properties and Applications. *Mater. Sci. Eng. R-Reports*, *43*, 61–102.

[9] **Harris, P. J. F.** (1999).*Carbon Nanotubes and Related Structures*. Cambridge University Press.

[10] **Meyyappan, M.** (2004).*Carbon Nanotubes: Science and Applications*. CRC Press.

[11] **Govindaraj, A.** (2005). *Nanotubes and Nanowires*. RSC Publications.

[12] **Dresselhaus, M. S., Dresselhaus, G., Avouris, P.** (2001). Eds., *Carbon Nanotubes*, *80*. Berlin, Heidelberg: Springer Berlin Heidelberg.

[13] **Iijima, S.** (1991). Helical microtubules of graphitic carbon. *Nature*, *354* (6348), 56–58.

[14] **Iijima S., and Ichihashi, T.** (1993). Single-shell carbon nanotubes of 1-nm diameter. *Nature*, *363* (6430), 603–605.

[15] **Yamabe, T.** (1995). Recent development of carbon nanotube. *Synth. Met.*, *70* (1–3), 1511–1518.

[16] **Terrones, M.** (2003). Science and technology of the twenty-first century: Synthesis, Properties, and Applications of Carbon Nanotubes. *Annu. Rev. Mater. Res.*, *33* (1), 419–501.

[17] **Saito, R., Dresselhaus G., Dresselhaus M. S.** (1998). *Physical properties of carbon nanotubes*. Imperial College Press, London.

[18] **Ouyang, M. J., Huang, L., Cheung, C. L., Lieber, C. M.** (2001). Energy gaps in 'metallic' single-walled carbon nanotubes. *Science*, *292* (5517), 702–5.

[19] **Dresselhaus, M. S., Dresselhaus, G., Saito, R.** (1992). Carbon fibers based on C60 and their symmetry. *Phys. Rev. B*, *45* (11), 6234–6242.

[20] **Chico, L., Crespi, V., Benedict, L., Louie, S., Cohen, M.** (1996). Pure carbon nanoscale devices: Nanotube heterojunctions. *Phys. Rev. Lett.*, *76* (6), 971–974.

[21] **Saito, R., Fujita, M., Dresselhaus, G., Dresselhaus, M. S.** (1992). Electronic structure of chiral graphene tubules. *Appl. Phys. Lett.*, *60* (18), 2204.

[22] **Miyauchi, Y., Oba, M., Maruyama, S.** (2006). Cross-polarized optical absorption of single-walled nanotubes by polarized photoluminescence excitation spectroscopy. *Phys. Rev. B*, *74* (20), 205440.

[23] **Kataura, H., Kumazawa, Y., Maniwa, Y., Umezu, I., Suzuki, S., Ohtsuka, Y., Achiba, Y.** (1999). Optical properties of single-wall carbon nanotubes. *Synth. Met.*, *103* (1–3), 2555–2558.

[24] **Fantini, C., Jorio, A., Souza, M., Strano, M. S., Dresselhaus, M. S., Pimenta, M. A.** (2004). Optical transition energies for carbon nanotubes from resonant Raman spectroscopy: environment and temperature effects. *Phys. Rev. Lett.*, *93* (14), 147406.

[25] **Dresselhaus, M. S., Dresselhaus, G., Saito, R., Jorio, A.** (2005). Raman spectroscopy of carbon nanotubes. *Phys. Rep.*, *409* (2), 47–99.

[26] **Farhat, S., Lamy de La Chapelle M., Loiseau, A., Scott, C. D., Lefrant, S., Journet C., Bernier, P.** (2001). Diameter control of single-walled carbon nanotubes using argon–helium mixture gases. *J. Chem. Phys.*, *115* (14), 6752.

[27] **Waldorff, E. I.** (2004). Characterization of carbon nanotubes produced by arc discharge: Effect of the background pressure. *J. Appl. Phys.*, *95* (5), 2749.

[28] **Bethune, D. S., Klang, C. H., de Vries, M. S., Gorman, G., Savoy, R., Vazquez, J., Beyers, R.** (1993). Cobalt-catalysed growth of carbon nanotubes with single-atomic-layer walls. *Nature*, *363* (6430), 605–607.

[29] **Endo, M., Takeuchi, K., Igarashi, S., Kobori, K., Shiraishi, M., Kroto, H. W.** (1993). The production and structure of pyrolytic carbon nanotubes (PCNTs). *J. Phys. Chem. Solids*, *54* (12), 1841–1848.

[30] **Guo, T., Nikolaev, P., Thess, A., Colbert, D. T., Smalley, R. E.** (1996). Catalytic growth of single-walled nanotubes by laser vaporization. *Chem. Phys. Let.*, *245*, 49-54.

[31] **O'Connel, M. J.** (2006). *Carbon nanotubes: Properties and Applications*. Florida: Taylor & Francis.

[32] **José-Yacamán, M., Miki-Yoshida, M., Rendón, L., Santiesteban, J. G.** (1993). Catalytic growth of carbon microtubules with fullerene structure, *Appl. Phys. Lett.*, *62* (2), 202.

[33] **Maruyama, S., Kojima, R., Miyauchi, Y., Chiashi, S., Kohno, M.** (2002). Low-temperature synthesis of high-purity single-walled carbon nanotubes from alcohol. *Chem. Phys. Lett.*, *360* (3–4), 229–234.

[34] **Mukhopadhyay, K., Koshio, A., Tanaka, N., Shinohara, H.** (1998). A Simple and Novel Way to Synthesize Aligned Nanotube Bundles at Low Temperature. *Jpn. J. Appl. Phys.*, *37* (2-10B), L1257–L1259.

[35] **Journet, C., Maser, W. K., Bernier, P., Loiseau, A., de la Chapelle M. L., Lefrant, S., Deniard, P., Lee, R., Fischer, J. E.** (1997). Large-scale production of single-walled carbon nanotubes by the electric-arc technique. *388* (6644), 756–758.

[36] **Colomer, J. F., Piedigrosso, P., Willems, I., Journet, C., Bernier, P., Van Tendeloo, G., Fonseca, A., Nagy, J. B.** (1998). Purification of catalytically produced multi-wall nanotubes. *J. Chem. Soc. Faraday Trans.*, *94* (24), 3753–3758.

[37] **Öncel Ç., and Yürüm, Y.** (2006). Carbon Nanotube Synthesis via the Catalytic CVD Method: A Review on the Effect of Reaction Parameters. *Fullerenes, Nanotub. Carbon Nanostructures*, *14* (1), 17–37.

[38] **Cheng, Q., Debnath, S., O'Neill, L., Hedderman, T. G., Gregan, E., Byrne, H. J.** (2010). Systematic Study of the Dispersion of SWNTs in Organic Solvents. *J. Phys. Chem. C*, *114* (11), 4857–4863.

[39] **Matarredona, O., Rhoads, H., Li, Z., Harwell, J. H., Balzano, L., Resasco, D. E.** (2003). Dispersion of Single-Walled Carbon Nanotubes in Aqueous Solutions of the Anionic Surfactant NaDDBS. *J. Phys. Chem. B*, *107* (48), 13357–13367.

[40] **Moore, V. C., Strano, M. S., Haroz, E. H., Hauge, R. H., Smalley, R. E., Schmidt, J., Talmon, Y.** (2003). Individually Suspended Single-Walled Carbon Nanotubes in Various Surfactants. *Nano Lett.*, *3* (10), 1379–1382.

[41] **Lay, M. D., Novak, J. P., Snow, E. S.** (2004). Simple Route to Large-Scale Ordered Arrays of Liquid-Deposited Carbon Nanotubes. *Nano Lett.*, *4* (4), 603–606.

[42] **Saran, N., Parikh, K., Suh, D. S., Muñoz, E., Kolla, H., Manohar, S. K.** (2004). Fabrication and characterization of thin films of single-walled carbon nanotube bundles on flexible plastic substrates. *J. Am. Chem. Soc.*, *126* (14), 4462–3.

[43] **Chen, J., Rao, A. M., Lyuksyutov, S., Itkis, M. E., Hamon, M. A., Hu, H., Cohn, R. W., Eklund, P. C., Colbert, D. T., Smalley, R. E., Haddon, R. C.** (2001). Dissolution of Full-Length Single-Walled Carbon Nanotubes. *J. Phys. Chem. B*, *105* (13), 2525–2528.

[44] **Kaempgen, M., Lebert, M., Haluska, M., Nicoloso, N., Roth, S.** (2008). Sonochemical Optimization of the Conductivity of Single Wall Carbon Nanotube Networks. *Adv. Mater.*, *20* (3), 616–620.

[45] **Bahr, J. L., Mickelson, E. T., Bronikowski, M. J., Smalley, R. E., Tour, J. M.** (2001). Dissolution of small diameter single-wall carbon nanotubes in organic solvents?. *Chem. Commun.*, *2*, 193–194.

[46] **Muhlbauer, R. L., Rosario, A.,** *A Review on the Synthesis of Carbon Nanotube Thin Films*, M. K. A., Ed. Nova science Publisher, (pp. 107–156).

[47] **Ham, H. T., Choi, Y. S., Jeong, N., Chung, I. J.** (2005). Single-wall carbon nanotubes covered with polypyrrole nanoparticles by the miniemulsion polymerization. *Polymer (Guildf).*, *46* (17), 6308–6315.

[48] **Strano, M. S., Dyke, C. A., Usrey, M. L., Barone, P. W., Allen, M. J., Shan, H., Kittrell, C., Hauge, R. H., Tour, J. M., Smalley, R. E.** (2003). Electronic structure control of single-walled carbon nanotube functionalization. *Science*, *301* (5639), 1519–22.

[49] **Yurekli, K., Mitchell, C. A., Krishnamoorti, R.** (2004). Small-angle neutron scattering from surfactant-assisted aqueous dispersions of carbon nanotubes. *J. Am. Chem. Soc.*, *126* (32), 9902–9903.

[50] **Islam, M. F., Rojas, E., Bergey, D. M., Johnson, A. T., Yodh, A. G.** (2003). High Weight Fraction Surfactant Solubilization of Single-Wall Carbon Nanotubes in Water. *Nano Lett.*, *3* (2), 269–273.

[51] **Banerjee, S., Hemraj-Benny, T., Wong, S. S.** (2005). Covalent Surface Chemistry of Single-Walled Carbon Nanotubes. *Adv. Mater.*, *17* (1), 17–29.

[52] **Tasis, D., Tagmatarchis, N., Bianco, A., Prato, M.** (2006). Chemistry of carbon nanotubes. *Chem. Rev.*, *106* (3), 1105–36.

[53] **Yu, X., Rajamani, R., Stelson, K. A., Cui, T.** (2008). Fabrication of carbon nanotube based transparent conductive thin films using layer-by-layer technology. *Surf. Coatings Technol.*, *202* (10), 2002–2007.

[54] **Yu, X., Rajamani, R., Stelson, K. A., Cui, T.** (2006). Carbon Nanotube Based Transparent Conductive Thin Films. *J. Nanosci. Nanotechnol.*, *6* (7), 1939–1944.

[55] **Ho X., and Wei, J.** (2013). Films of Carbon Nanomaterials for Transparent Conductors. *Materials (Basel).*, *6* (6), 2155–2181.

[56] **Andrew Ng, M. H., Hartadi, L. T., Tan, H., Patrick Poa, C. H.** (2008). Efficient coating of transparent and conductive carbon nanotube thin films on plastic substrates. *Nanotechnology*, *19* (20), 205703.

[57] **Majumder, M., Rendall, C., Li, M., Behabtu, N., Eukel, J. A., Hauge, R. H., Schmidt, H. K., Pasquali, M.** (2010). Insights into the physics of spray coating of SWNT films. *Chem. Eng. Sci.*, *65* (6), 2000–2008.

[58] **Jung, H., Van Quy, N., Hoa, N. D., Kim, D.** (2010). Transparent Field Emission Device from a Spray Coating of Single-Wall Carbon Nanotubes. *J. Electrochem. Soc.*, *157* (11), J371.

[59] **Maeda, Y., Komoriya, K., Sode, K., Higo, J., Nakamura, T., Yamada, M., Hasegawa, T., Akasaka, T., Saito, T., Lu, J., Nagase, S.** (2011). Preparation and characterization of transparent and conductive thin films of single-walled carbon nanotubes. *Nanoscale*, *3* (4), 1904–9.

[60] **Schindler, A., Brill, J., Fruehauf, N., Novak, J. P., Yaniv, Z.** (2007). Solution-deposited carbon nanotube layers for flexible display applications. *Phys. E Low-dimensional Syst. Nanostructures*, *37* (1–2), 119–123.

[61] **Scardaci, V., Coull, R., Coleman, J. N.** (2010). Very thin transparent, conductive carbon nanotube films on flexible substrates. *Appl. Phys. Lett.*, *97* (2), 023114.

[62] **Liu, Q., Fujigaya, T., Cheng, H. M., Nakashima, N.** (2010). Free-standing highly conductive transparent ultrathin single-walled carbon nanotube films. *J. Am. Chem. Soc.*, *132* (46), 16581–6.

[63] **Tenent, R. C., Barnes, T. M., Bergeson, J. D., Ferguson, A. J., To, B., Gedvilas, L. M., Heben, M. J., Blackburn, J. L.** (2009). Ultrasmooth, Large-Area, High-Uniformity, Conductive Transparent Single-Walled-Carbon-Nanotube Films for Photovoltaics Produced by Ultrasonic Spraying. *Adv. Mater.*, *21* (31), 3210–3216.

[64] **Faure, B., Salazar-Alvarez, G., Ahniyaz, A., Villaluenga, I., Berriozabal, G., De Miguel, Y. R., Bergström, L.** (2013). Dispersion and surface functionalization of oxide nanoparticles for transparent photocatalytic and UV-protecting coatings and sunscreens. *Sci. Technol. Adv. Mater.*, *14* (2), 023001.

[65] **Seo, M. A., Yim, J. H., Ahn, Y. H., Rotermund, F., Kim, D. S., Lee, S., Lim, H.** (2008). Terahertz electromagnetic interference shielding using single-walled carbon nanotube flexible films. *Appl. Phys. Lett.*, *93* (23), 231905.

[66] **Yim, J. H., Kim, Y. S., Koh, K. H., Lee, S.** (2008). Fabrication of transparent single wall carbon nanotube films with low sheet resistance. *J. Vac. Sci. Technol. B Microelectron. Nanom. Struct.*, *26* (2), 851.

[67] **Cao, Q., and Rogers, J. A.** (2009). Ultrathin Films of Single-Walled Carbon Nanotubes for Electronics and Sensors: A Review of Fundamental and Applied Aspects. *Adv. Mater.*, *21* (1), 29–53.

[68] **Wu, Z.** (2004). Transparent, Conductive Carbon Nanotube Films. *Science (80).*, *305* (5688), 1273–1276.

[69] **Chhowalla, M.** (2007). Transparent and conducting SWNT thin films for flexible electronics. *J. Soc. Inf. Disp.*, *15* (12), 1085.

[70] **Barnes, T. M., Lagemaat, J., Levi, D., Rumbles, G., Coutts, T. J., Weeks, C. L., Britz, D. A., Levitsky, I., Peltola, J., Glatkowski, P.** (2007). Optical characterization of highly conductive single-wall carbon-nanotube transparent electrodes. *Phys. Rev. B*, *75* (23), 235410.

[71] **Nirmalraj, P. N., Lyons, P. E., De, S., Coleman, J. N., Boland, J. J.** (2009). Electrical connectivity in single-walled carbon nanotube networks. *Nano Lett.*, *9* (11), 3890–5.

[72] **Barnes, T. M., Blackburn, J. L., Lagemaat, J., Coutts, T. J., Heben, M. J.** (2008). Reversibility, dopant desorption, and tunneling in the temperature-dependent conductivity of type-separated, conductive carbon nanotube networks. *ACS Nano*, *2* (9), 1968–76.

[73] **Blackburn, J. L., Barnes, T. M., Beard, M. C., Kim, Y. H., Tenent, R. C., McDonald, T. J., To, B., Coutts, T. J., Heben, M. J.** (2008). Transparent conductive single-walled carbon nanotube networks with precisely tunable ratios of semiconducting and metallic nanotubes. *ACS Nano*, *2* (6), 1266–74.

[74] **Jackson, R., Domercq, B., Jain, R., Kippelen, B., Graham, S.** (2008). Stability of Doped Transparent Carbon Nanotube Electrodes. *Adv. Funct. Mater.*, *18* (17), 2548–2554.

[75] **Gordon, R. G.** (2011). Criteria for Choosing Transparent Conductors. *MRS Bull.*, *25* (08), 52–57.

[76] **Barnes, T. M., Reese, M. O., Bergeson, J. D., Larsen, B. A., Blackburn, J. L., Beard, M. C., Bult, J., Lagemaat, J.** (2012). Comparing the Fundamental Physics and Device Performance of Transparent, Conductive Nanostructured Networks with Conventional Transparent Conducting Oxides. *Adv. Energy Mater.*, *2* (3), 353–360.

[77] **Bekyarova, E., Itkis, M. E., Cabrera, N., Zhao, B., Yu, A., Gao, J., Haddon, R. C.** (2005). Electronic properties of single-walled carbon nanotube networks. *J. Am. Chem. Soc.*, *127* (16), 5990–5.

[78] **Kymakis, E., Stratakis, E., Koudoumas, E.** (2007). Integration of carbon nanotubes as hole transport electrode in polymer/fullerene bulk heterojunction solar cells. *Thin Solid Films*, *515* (24), 8598–8600.

[79] **Zhang, H. W., and Xu, W.** (1992). Effect of bias and post-deposition vacuum annealing on structure and transmittance of ITO films. *Vacuum*, *43* (8), 835–836.

[80] **Lewis, B. G., and Paine, D. C.** (2011). Applications and Processing of Transparent Conducting Oxides. *MRS Bull.*, *25* (08), 22–27.

[81] **Zhou, Y. , Hu, L., Grüner, G.** (2006). A method of printing carbon nanotube thin films. *Appl. Phys. Lett.*, *88* (12), 123109.

[82] **Jung de Andrade, M., Dias Lima, M., Skákalová, V., Pérez Bergmann, C., Roth, S.** (2007). Electrical properties of transparent carbon nanotube networks prepared through different techniques. *Phys. status solidi – Rapid Res. Lett.*, *1* (5), 178–180.

[83] **Li, J., Hu, L., Wang, L., Zhou, Y., Grüner, G., Marks, T. J.** (2006). Organic light-emitting diodes having carbon nanotube anodes. *Nano Lett.*, *6*, (11), 2472–7.

[84] **Zhang, D. H., Ryu, K., Liu, X. L., Polikarpov, E., Ly, J., Tompson, M. E., Zhou, C. W.** (2006). Transparent, conductive, and flexible carbon nanotube films and their application in organic light-emitting diodes. *Nano Lett.*, *6* (9), 1880–1886.

[85] **Aguirre, C. M., Auvray, S., Pigeon, S., Izquierdo, R., Desjardins, P., Martel, R.** (2006). Carbon nanotube sheets as electrodes in organic light-emitting diodes. *Appl. Phys. Lett.*, *88* (18), 183104.

[86] **Li, Z., Kandel, H. R., Dervishi, E., Saini, V., Xu, Y., Biris, A. R., Lupu, D., Salamo, G. J., Biris, A. S.** (2008). Comparative study on different

carbon nanotube materials in terms of transparent conductive coatings. *Langmuir*, *24* (6), 2655–62.

[87] **Geng, H. Z., Kim, K. K., Lee, K., Kim, G. Y., Choi, H. K., Lee, D. S., An, K. H., Lee, Y. H., Chang, Y., Lee, Y. S., Kim, B., Lee, Y. J.** (2007). Dependence of material quality on performance of flexible transparent conducting films with single-walled carbon nanotubes. *Nano*, *02* (03), 157–167.

[88] **Kaskela, A., Nasibulin, A. G., Timmermans, M. Y., Aitchison, B., Papadimitratos, A., Tian, Y., Zhu, Z., Jiang, H., Brown, D. P., Zakhidov, A., Kauppinen, E. I.** (2010). Aerosol-synthesized SWCNT networks with tunable conductivity and transparency by a dry transfer technique. *Nano Lett.*, *10* (11), 4349–55.

[89] **Shin, D. H., Shim, H. C., Song, J. W., Kim, S., Han, C. S.** (2009). Conductivity of films made from single-walled carbon nanotubes in terms of bundle diameter. *Scr. Mater.*, *60* (8), 607–610.

[90] **Znidarsic, A., Kaskela, A., Laiho, P., Gaberscek, M., Ohno, Y., Nasibulin, A. G., Kauppinen, E. I., Hassanien, A.** (2013). Spatially Resolved Transport Properties of Pristine and Doped Single-Walled Carbon Nanotube Networks. *J. Phys. Chem. C*, *117* (25), 13324–13330.

[91] **Geng, H. Z., Lee, D. S., Kim, K. K., Kim, S. J., Bae, J. J., Lee, Y. H.** (2008). Effect of Carbon Nanotube Types in Fabricating Flexible Transparent Conducting Films. *J. Korean Phys. Soc.*, *53* (92), 979.

[92] **Shim, B. S., Tang, Z., Morabito, M. P., Agarwal, A., Hong, H., Kotov, N. A.** (2007). Integration of Conductivity, Transparency, and Mechanical Strength into Highly Homogeneous Layer-by-Layer Composites of Single-Walled Carbon Nanotubes for Optoelectronics. *Chem. Mater.*, *19* (23), 5467–5474.

CURRICULUM VITAE

Name Surname: Fatma ÇOLAK

Place and Date of Birth: Bulgaria-06.12.1987

E-Mail: fcolak@itu.edu.tr

EDUCATION:

B.Sc.: 2012, Yildiz Technical University, Faculty of Chemical and Metallurgical Engineering, Chemical Engineering